

Anna Tilp, BSc

The Contribution of Adipocyte Hormone Sensitive Lipase to Glucose, Energy, and Lipid Homeostasis

MASTERARBEIT

zur Erlangung des akademischen Grades

Master of Science

Masterstudium Biochemie und Molekulare Biomedizin

eingereicht an der

Technischen Universität Graz

Betreuerin

Mag. Dr.rer.nat. Gabriele Schoiswohl

Institut für molekulare Biowissenschaften

KFU Graz

EIDESSTATTLICHE ERKLÄRUNG

Ich erkläre an Eides statt, dass ich die vorliegende Arbeit selbstständig verfasst, andere als die angegebenen Quellen/Hilfsmittel nicht benutzt, und die den benutzten Quellen wörtlich und inhaltlich entnommenen Stellen als solche kenntlich gemacht habe. Das in TUGRAZonline hochgeladene Textdokument ist mit der vorliegenden Masterarbeit identisch.

Datum

Unterschrift

Table of Contents

Abstract	5
Zusammenfassung.....	6
Danksagung	7
1. Introduction	8
1.1 Adipose Tissue	8
White Adipose Tissue	9
Brown Adipose Tissue	9
1.2 Adipocyte Differentiation.....	10
1.3 Adipocyte Metabolism	12
Lipid Metabolism.....	12
Intracellular Lipolysis.....	14
Regulation of Intracellular Lipolysis	16
Glucose Metabolism.....	18
1.4 Adipokine Secretion	19
1.5 The Aim of the Thesis	21
2. Materials	22
2.1 Plastic and Hardware.....	22
2.2 Chemicals.....	22
2.3 Equipment	22
2.4 Buffer and Solutions	23
Cell Culture, Protein, and RNA Isolation.....	23
SDS Gel electrophoresis and Western Blot	23
ORO Staining and TLC Analysis	24
2.5 Media.....	25
2.6 Kits	25
Quantitative Polymerase Chain Reaction.....	25
Determination of Free Fatty Acids and Glycerol	25
BCA Protein Determination	25
2.7 Western Blot Analysis.....	25
Primary and Secondary Antibodies	26
Primary Antibodies.....	26
Secondary Antibodies.....	26

2.8	Real Time PCR Primer	27
3.	Methods	28
3.1	Western Blot Analysis.....	28
	Protein Isolation from Adipose Tissues (total homogenate)	28
	Protein Isolation from Cells	28
	Determination of Protein Concentration	28
	SDS-Gel electrophoresis and Membrane Transfer.....	28
3.2	RNA Isolation and cDNA synthesis	29
3.3	Quantitative Real-Time PCR (RT-PCR)	29
3.4	Animals	30
3.5	Determination of Plasma Lipid Parameters	30
	NEFA determination	30
	Glycerol determination	30
3.6	Primary Cell Culture.....	30
	Isolation of SVC.....	31
	Differentiation of Adipocytes	31
3.7	Oil Red O Staining (ORO)	31
3.8	Thin Layer Chromatography	32
3.9	Radioactive Assays.....	32
	<i>In Vitro</i> Glucose Uptake.....	32
	<i>In Vitro</i> Fatty Acid Uptake	32
	<i>In vivo</i> Glucose and Bromo-Palmitate Uptake	33
	<i>In vivo</i> Oleic Acid Uptake.....	33
3.10	Statistics.....	33
4.	Results	34
4.1	Consequences of Adipocyte Specific HSL deletion <i>in vitro</i>	34
	Adipocyte Differentiation.....	34
	Adipocyte Function	38
4.2	Consequences of Adipocyte Specific HSL Deletion <i>in vivo</i>	41
	AT Function and Health in AHKO mice	41
	Investigation of Systemic Glucose and Lipid Metabolism in AHKO mice	47
5.	Discussion	50
	Abbreviations	55
	References.....	56

Abstract

Adipose tissue (AT) plays a critical role in maintaining metabolic homeostasis, not only through its ability to store and mobilize energy as lipids, but also *via* its role as an endocrine organ. Dysregulations in fat storage and/or degradation of lipids are related to pathogenesis and the development of severe metabolic diseases like obesity, dyslipidemia, insulin resistance or hepatic steatosis. Lipolysis describes the breakdown of triacylglycerols (TAGs) to release free fatty acids (FFAs) along with the glycerol backbone. This process is predominantly catalyzed by adipose triglyceride lipase (ATGL) and hormone-sensitive lipase (HSL), the main TG hydrolases in AT. While the role of ATGL has been studied excessively during the last years, the contribution of adipocyte specific HSL to the development of metabolic diseases is still controversial. The aim of this master thesis is to enlighten the function of adipocyte specific HSL to both adipose tissue and systemic energy and glucose homeostasis. For this purpose, we used a mouse model with the specific deletion of HSL in adipocytes referred here as AHKO mice. These mice express Cre recombinase under control of the mouse adiponectin (Adipoq) promoter along with a LoxP flanked (floxed) HSL gene resulting in a specific deletion of HSL in mature white and brown adipocytes, but not macrophages.

The experimental approach of this master thesis was structured into two parts: 1) Cellular impact of HSL loss on adipocyte differentiation and function using primary cells isolated from subcutaneous AT (SCAT) of AHKO and control mice. 2) The contribution of adipocyte HSL deletion to AT function and health as well as systemic lipid and glucose homeostasis in mice.

Cell culture experiments indicated that deletion of HSL in mature adipocytes did not affect storage of neutral lipids and expression of transcription factors involved in adipogenesis suggesting adequate adipocyte differentiation ability. Furthermore, primary AHKO adipocytes showed no impairments in critical adipocyte function such as glucose and lipid uptake. However, these observations could not be directly translated to AHKO mice. WAT depots of AHKO mice did not expand in accordance with control littermates resulting in a lipodystrophic phenotype. The reduced AT mass was accompanied with dysregulations in lipid metabolism including lipid uptake, synthesis, and storage as well as lipolysis. Furthermore, increased infiltration of immune cells indicated impaired AT health in AHKO mice. Together, deletion of adipocyte HSL progressively deteriorate AT function and health *in vivo* which consequently affect systemic lipid and glucose homeostasis.

Zusammenfassung

Fettgewebe gehört zu den wichtigsten Organen zur Erhaltung des metabolischen Gleichgewichts des Körpers. Dies geschieht nicht nur durch die Fähigkeit überschüssige Energie in Form von Triacylglyceriden (TAGs) zu speichern, sondern auch durch die Beteiligung als wichtiges endokrines Organ für die Synthese und die Sekretion von bioaktiven Proteinen und Hormonen, sogenannten Adipokinen. Veränderungen im Aufbau und/oder der Mobilisierung von Lipidreservoirs stehen im engen Zusammenhang mit der Entstehung von Krankheiten wie Fettleibigkeit, Dyslipidämie, Insulin-Resistenz oder Lebersteatose. Lipolyse beschreibt den Prozess der stufenweisen Esterspaltung der TAG Speicher, wobei freie Fettsäuren (FFS) und Glycerol entstehen. Die Hydrolyse intrazellulärer Fettspeicher wird hauptsächlich von zwei Lipasen, der Adipozyten-Triglyzerid-Lipase (ATGL) und der Hormon-Sensitiven-Lipase (HSL), katalysiert. Während die Rolle von ATGL in den letzten Jahren in vielen Studien untersucht wurde, ist die Beteiligung der adipozyten-spezifischen HSL noch immer umstritten. In dieser Masterarbeit wird die Beteiligung der adipozyten-spezifischen HSL zum fettgewebsspezifischen Stoffwechsel und die daraus resultierenden Konsequenzen auf den systemischen Energie- und Glukosemetabolismus untersucht. Um dieses Ziel zu erreichen, arbeiteten wir mit einem Mausmodell, in dem HSL spezifisch in reifen Adipozyten deletiert wurde. Die sogenannte AHKO-Maus exprimiert die Cre-Rekombinase unter der Kontrolle des Maus Adiponektin Promoters in Kombination mit einem von LoxP eingeschlossenem (floxed) HSL Gen. Dies führt zur gezielten Entfernung von HSL in Adipozyten des weißen und braunen Fettgewebes, nicht aber in Makrophagen.

Die Masterarbeit wurden in zwei Teile gegliedert: 1) Die Auswirkungen des zellulären Verlustes von HSL auf den Differenzierungsvorgang von primären Zellen aus subkutanem AT (SCAT) von AHKO und Kontroll-Mäusen sowie deren primäre Zellfunktionen. 2) Die Beteiligung des adipozyten-spezifischen HSL Verlustes zu AT Funktion und Gesundheit sowie die Auswirkungen auf den systemischen Lipid- und Glucosestoffwechsel in Mäusen.

In den Zellkultur Experimenten verhielten sich primäre AHKO-Zellen analog zu Kontrollzellen mit angemessener Neutrallipidakkumulation und einer vergleichbaren Expression von Transkriptionsfaktoren, die für den Differenzierungsvorgang von pluripotenten Präadipozyten zu reifen Adipozyten verantwortlich sind. Auch wurden keine Unterschiede in kritischen Zellfunktionen wie Glukose- oder Lipidaufnahme zwischen AHKO und Kontrollzellen beobachtet. Diese Resultate können jedoch nicht direkt in die *in vivo* Situation und die Fettgewebefunktion übertragen werden. Weißes Fettgewebe von AHKO Mäusen entwickelte sich nicht im Einklang mit Kontrolltieren. Die fehlende Zunahme des Fettgewebes wurde von Dysregulationen im Lipidstoffwechsel, inklusive Lipidaufnahme, -synthese und -speicherung, und der Herunterregulierung von lipolytischen Proteinen begleitet. Weiters wurde die Einwanderung von Immunzellen ins Fettgewebe von AHKO Mäusen beobachtet. Zusammenfassend resultiert die adipozyten-spezifische Deletion von HSL in zunehmender Verschlechterung von AT Funktion und Gesundheit, mit Auswirkungen auf den systemischen Lipid- und Glukosestoffwechsel *in vivo*.

Danksagung

Mein größter Dank gilt meiner Betreuerin, Gabriele Schoiswohl. Liebe Gabi, danke für deine Unterstützung, deinen Rat, deine Geduld und deinen stetigen Optimismus. Dafür, dass du dir so viel Zeit genommen hast, immer ein offenes Ohr für mich hattest und eine Lösung für jedes Problem. Danke, dass ich so viel von dir lernen durfte und für all deine Ratschläge! Danke auch an Laura, für deine Hilfe bei den Experimenten und die schönen Stunden im Isotopenlabor. Die Zeit ist viel zu schnell vergangen, ich hätte mir keine bessere Arbeitsgruppe wünschen können! #WeLoveHSL

Weiters möchte ich mich bei der AG Radner bedanken. Lieber Franz, liebe Margarita, danke, dass ihr mit mir Büro und Laborplatz geteilt habt. Aber vor allem, danke für die schöne Zeit beim gemeinsamen Wandern, Schokolade essen und unseren unvergesslichen Feiern!

Danke auch an alle KollegInnen und FreundInnen am Institut für molekulare Biowissenschaften. Für die angenehme Arbeitsatmosphäre, eure Unterstützung im Labor, aber auch darüber hinaus! Danke für die vielen Gespräche, in denen der Spaß nie zu kurz kam. Danke für die schöne Zeit am Institut.

Ein besonderer Dank gilt auch meinen StudienkollegInnen und Freunden, die mit mir gemeinsam den Prüfungsstress überwunden haben und mich stets motiviert haben. Danke, für unsere gemeinsamen Erlebnisse und eure Unterstützung!

Lieber Alex, danke dir für deinen Rückhalt, dass ich mich immer auf dich verlassen kann und unsere schöne gemeinsame Zeit!

Ein großer Dank gilt auch meinen Eltern und meinen Geschwistern, die mich immer unterstützt haben und für mich da sind!

1. Introduction

The correlation between energy uptake and energy expenditure provides the foundation for a balanced energy metabolism and is closely associated with individual health. In this context, adipose tissue (AT) is critically involved in the development of metabolic diseases, with either abnormal accumulation of lipid stores in obese individuals or AT wasting as consequence of cancer or autoimmune diseases. Obesity reflects one of the main health problems of today's society as it provides the origin of the development of further medical complications including type 2 diabetes, cardiovascular, and liver diseases as well as cancer, causing more deaths worldwide than underweight does [1]. Obesity is characterized through massive accumulation of fat that is associated with disadvantages for the individual health and is classified through the body mass index (kg/m^2) in overweight ($\text{BMI} > 25$) and obese patients ($\text{BMI} > 30$). Besides genetic preposition, the main risk factors of obesity are lack of physical activity combined with unhealthy diets and the consumption of alcohol and/or tobacco.

Lipodystrophy belongs to a group of rare metabolic disease with either total or partial loss of AT mass. In contrast to cachexia, it describes the continuous loss rather than an acute loss of AT depots. Dysregulation of several genes have been identified to be associated with the development of lipodystrophy, e.g. 1-acylglycerol-3-phosphate O-acyltransferase 2 (AGPAT2) or perilipin 1 (PLIN1), proteins involved in the formation of triacylglycerols (TAGs) and the association to lipid droplets (LDs), respectively [2]. Besides genetic backgrounds, autoimmune diseases or drug treatment are associated with pathological AT reduction [2].

Both obesity and lipodystrophy show increased levels of circulating free fatty acids (FFA) either due to excessive loading of lipid stores or defective storage in adipocytes. This leads to an accumulation of lipids in non-ATs with associated problems and pathogenesis. Since the impact of AT dysregulations is not restricted to AT function but implicates disadvantages for systemic homeostasis, investigation of AT function and the cross talk to non-ATs provides important insights in the understanding of metabolic diseases and the development of new strategies for their treatment.

1.1 Adipose Tissue

AT represents a central organ for the systemic homeostasis of glucose and lipid metabolism within the body. Specialized AT depots are distributed within the whole body and serve as energy reservoir, embedment for organs, insulation, and maintenance of body temperature. Furthermore, AT is involved in the synthesis and the secretion of important signaling molecules that are involved in systemic energy homeostasis, immune response, and hormone metabolism. Therefore, AT plays an indispensable role for the maintenance of systemic metabolic functions and provides an important origin for the understanding of the development of metabolic disorders.

Fat cells or adipocytes are the main cells found in AT. Along with preadipocytes, immune cells such as macrophages, and endothelial cells they built up this heterogenic organ. Adipocytes are capable to store neutral lipids such as TAGs, sterol esters, and wax esters in specialized compartments within the adipocyte. These LDs are organized as organelle vesicles surrounded by a phospholipid monolayer associated with membrane proteins and a neutral fat depot core [3]. Although LDs are present in most

cells, sizes, and number as well as fat composition and protein distribution differ between cell types and individual cells of the same kind according to their function, respectively. Lipid reservoirs provide the most effective form of energy storage within our body. Lipid energy reservoirs are mobilized in times of nutrient deprivation and stored upon nutritional abundance. In addition to energy substrate, the released FFA serve as important precursor and signaling molecules and building blocks for biological membranes and are therefore indispensable for the maintenance of normal metabolic processes within the body.

According to its macroscopic appearance as well as molecular properties and function, AT can be divided into two main groups: white and brown AT (**Figure 1**). In addition, there is an intermediate form between white and brown adipocytes referred as beige or brite AT.

White Adipose Tissue

White AT (WAT) depots are distributed within the whole body and can be classified according to their location in subcutaneous (SC) and visceral AT. SCAT is located under the skin of the whole body, with special depots in the abdominal, gluteal, and femoral region. Visceral AT is predominantly surrounding inner organs including intestines (omental fat and mesenteric), the kidneys (retroperitoneal) or the heart (epicardial) [4].

White adipocytes are characterized through a large LD (unilocular), forcing the remaining cytoplasm and the nucleus to the edge of the cell. The main task of these cells is the storage and release of FAs to provide a proper energy supply for the organism. However, AT represents not only a passive energy depot, but also an important endocrine organ involved in the synthesis and secretion of several hormones, bioactive proteins, and cytokines [5].

The location of the AT depot is closely related to its function. Depots differ in cellular properties including adipokine secretion, lipolytic activity as well as the expression of respective receptors. Compared to visceral fat, SCAT is referred to as relatively inert depot with lower lipolytic activity, thereby serving as buffer system to protect against lipotoxicity and lipid accumulation in non-AT depots [4]. Consequently, SCAT is associated with beneficial effects on systemic metabolism while visceral AT is associated with pathogenesis including metabolic syndrome [5], [6].

Brown Adipose Tissue

Brown AT (BAT) depots are distinct depots in rodents with defined anatomical locations. BAT depots in larger mammals, including humans, are increased neonatal and during early childhood, and less prominent in adult individuals. In adult humans, BAT depots are mainly found around the kidneys, the heart, and the aorta as well as neck, shoulder, and spine [7]. Adipocytes found in brown AT differ from white adipocytes in both their morphology and function. They are smaller (10-25 μm compared to 30-150 μm of white adipocytes) and are characterized through a round nucleus and the assembling of several, small LDs (multilocular). In addition, numerous large mitochondria are present within the cytoplasm. Together with an increased blood supply they are responsible for the typical brown color [7]. Unlike white adipocytes, the main function of brown adipocytes is thermogenesis, hence the production of heat during cold exposure, a process called non-shivering thermogenesis [7]. The typical

protein involved in this process is uncoupling protein 1 (UCP1) leading to an uncoupling of oxidative phosphorylation of ATP to generate heat. Despite heat generation, BAT is also involved in the secretion of adipokines, also referred as brown adipokines such as fibroblast growth factor-21 (FGF-21) [8]. Cold exposure or β -adrenergic stimulation increase the of UCP1 expression, causing an browning effect of white adipocytes [9].

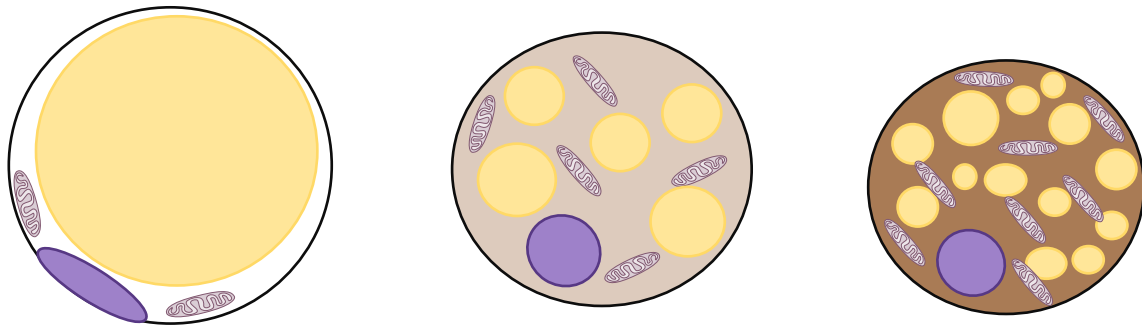


Figure 1: Morphological Differences of White, Brown, and Brite Adipocytes. Adipocytes can be classified according to their morphological appearance as well as their molecular function. Left: White adipocyte with large unilocular lipid droplet. Right: Brown adipocyte with high mitochondrial density and small, multilocular lipid droplets. Middle: brite adipocyte, an intermediate cell type.

1.2 Adipocyte Differentiation

The differentiation of progenitor cells to mature adipocytes is characterized by alternations in the expression pattern of genes that are responsible for the manifestation of the adipocyte phenotype, including both morphology and cellular metabolism. The initiation of adipogenesis requires the contribution and interaction of hormone signals as well as the activation of several groups of transcription factors. Three families of transcription factors have been identified to play a crucial role in the initiation and the maintenance of adipogenesis: CCAAT/ enhancer-binding proteins (C/EBPs), sterol regulatory binding protein (SREBP1c) and peroxisome proliferator-activated receptor γ (PPAR γ), the latter is attributed as key regulator of the process [10].

During differentiation, cells develop characteristic properties of adipocyte function, including lipid uptake and storage as well as insulin sensitivity. Promoters of major genes involved in adipocyte function have been found to provide binding sites for PPAR γ and C/EBP α . This includes glucose transporter (GLUT 4), lipoprotein lipase (LPL), and fatty acid synthase (FASN) [11], [12]. **Figure 2** provides a schematic overview on the expression pattern of transcription factors responsible to induce and maintain the differentiation process from precursor cells to mature adipocytes.

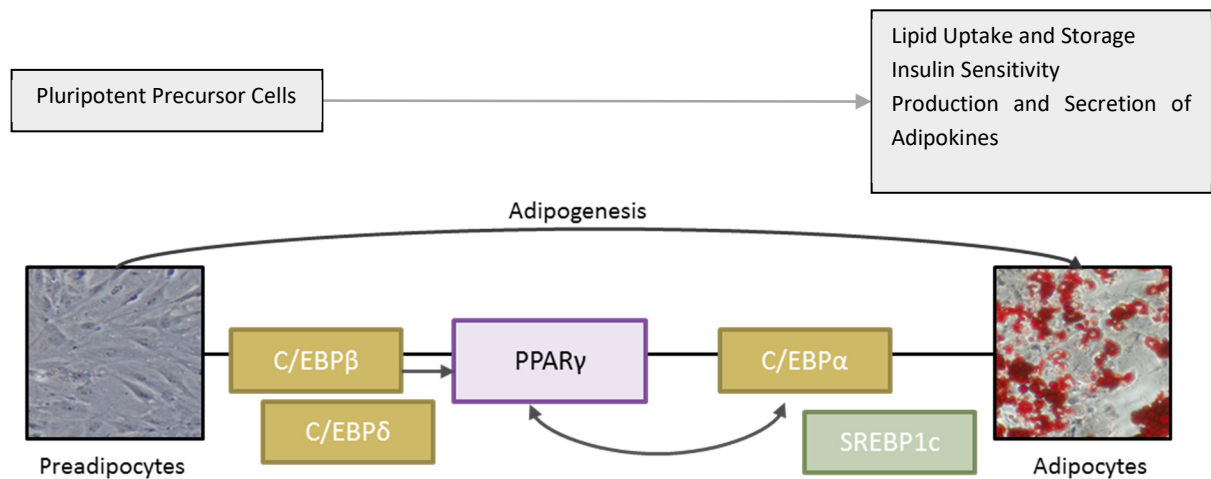


Figure 2: Schematic Overview of the Differentiation Process from Multipotent Precursor Cells to Mature Adipocytes with Distinct Properties. The process of adipogenesis is characterized through changes in the cellular expression pattern resulting in an adipogenic phenotype with lipid storage capacity. Introduction and maintenance of this process requires the activation of several transcription factors including C/EBPs, SREBPs, and PPAR γ which are expressed in a defined time course during adipogenesis.

C/EBP proteins represent an important family of transcription factors, sharing a highly conserved basic leucine zipper structure responsible for dimerization and DNA binding to the CCAAT box motif within the promoters of target genes. During early stages of adipogenesis, the expression of two isoforms, C/EBP β and C/EBP δ , are reported whereas C/EBP α is expressed in the late phase of differentiation. The main function of C/EBP β and C/EBP δ is the induction of PPAR γ and C/EBP α expression [13], [14]. C/EBP α was found to induce the expression of genes characterizing the adipose phenotype as well as to give positive feedback to stimulate PPAR γ expression [14]. The importance of C/EBP β and C/EBP δ for adipogenesis was demonstrated in knockout mice models. Animals lacking both C/EBP β and C/EBP δ displayed increased rates of prenatal death and surviving animals showed dysregulations in the formation of neutral lipid stores in white and brown AT depots despite a normal expression of PPAR γ and C/EBP α [15], indicating a critical role of C/EBPs beside the activation of PPAR γ .

SREBP1c or adipocyte determination and differentiation factor-1 (ADD-1) belongs to the basic helix-loop-helix-leucine zipper (bHLH-Zip) family of transcription factors [16]. It is predominantly expressed during the late phase of adipogenesis and is known to enhance PPAR γ action through inducing its expression levels as well as providing ligands for binding and enhancing PPAR γ activity [11].

PPARs belong to the family of nuclear hormone receptors and their activity is induced through binding of their respective ligands. Three isoforms of PPARs are known: PPAR α , PPAR β , and PPAR γ . While PPAR α and PPAR β are predominantly involved in lipid oxidation, PPAR γ was found to play a crucial role in adipocyte development, where it is addressed as key regulator [10], [12], [17]. Polyunsaturated fatty acids as well as specific synthetic compounds from the group of thiazolidinediones are known substrates of PPAR γ [12]. Upon activation, PPAR γ build heterodimers with the retinoid X receptor (RXR) thereby controlling the transcription of various genes involved in fundamental metabolic processes including glucose and lipid homeostasis. *In vivo* studies revealed that mice homozygote for PPAR γ knockout die during embryonal development due to impaired placentar development [18]. The importance of PPAR γ for adipocyte development was demonstrated in mice with targeted deletion of PPAR γ in adipocytes. These animals revealed dysregulations in AT development, function, and increased lipid deposition in the liver [19].

1.3 Adipocyte Metabolism

Adipocytes are specialized cells to serve as lipid reservoir for energy production and the supply with precursor and signaling molecules. The metabolic features of adipocytes differ between AT depots and are dependent on dietary status as well as hormonal status of the individual.

Adipocyte function includes synthesis and uptake of extracellular FA to generate lipids such as TAG, mobilization of these TAG stores (i.e. TAG hydrolysis or lipolysis) upon nutritional demand as well as glucose uptake upon insulin stimulation and adipokine synthesis and secretion.

Lipid Metabolism

TAG formation

TAG stores represent the most prominent and efficient storage of energy in eukaryotic organisms. Except for erythrocytes, all cells are capable of synthesizing TAGs to build up cellular lipid stores. However, AT depots are the main source of energy since adipocytes are specialized to store energy in form of TAGs within characteristic cell compartments, the LDs.

Two different pathways are described for TAG synthesis: the glycerol pathway and the monoacylglycerol pathway [20] (**Figure 3**).

Before entering the glycerol pathway, FA and the glycerol moiety need to be converted to their active forms, Acyl-CoA, and glycerol-3-phosphate (G3P). These reactions are catalyzed through acyl-CoA-synthetase (ACC) and glycerin-3-phosphatedehydrogenase, respectively. Most cells are capable of producing TAGs through the glycerol pathway. The first step within this pathway is catalyzed through glycerol-3-phosphate-acyltransferase (GPAT) and provides the linkage between the G3P backbone and an acyl-CoA moiety resulting in lysophosphatidate. After the attachment of a second acyl-CoA group through lysophosphatidate-acyltransferase (AGPAT), the phosphate group is released resulting in a 1,2-diacylglycerol (DAG) via phosphatidic acid phosphohydrolase (PAP) activity. The last step in TAG formation is catalyzed through diacylglycerol-acyltransferase (DGAT), connecting the third acyl-CoA residue to the glycerol backbone [20].

The monoacylglycerol (MAG) pathway is especially important for lipid resorption in the small intestine and is abundant in enterocytes and hepatocytes [21]. This pathway includes the acylation of MAGs through monoacylglycerol-acyltransferase (MGAT). The resulting DAG is again converted into TAG through a DGAT catalyzed reaction [20].

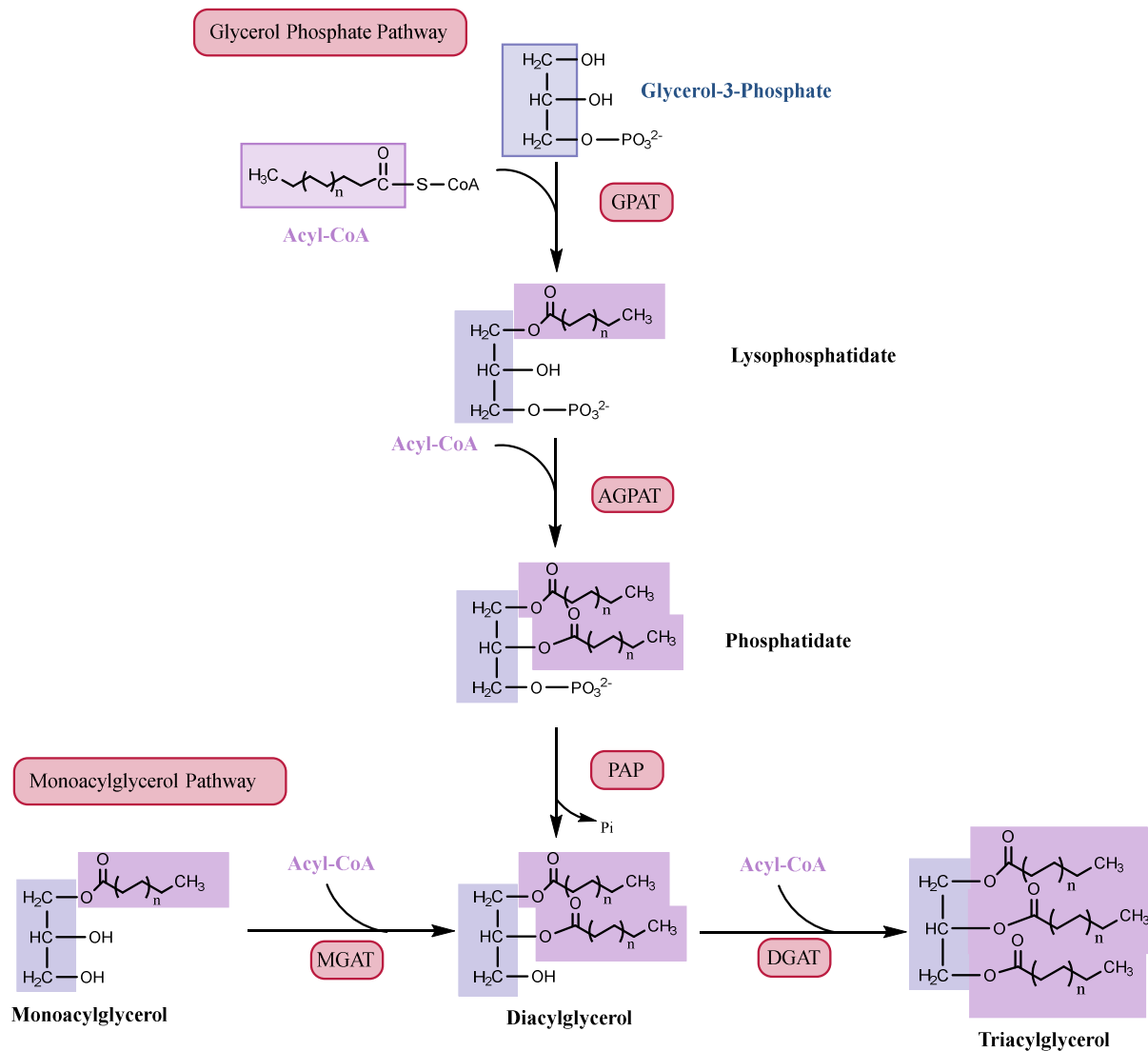


Figure 3: Schematic Illustration of Triacylglycerol Synthesis. The synthesis of TAG species requires activated glycerol and fatty acid species, respectively. Two pathways are illustrated in this scheme: the glycerol-3-phosphate pathway describes the de novo synthesis of TAGs, which is prominent in the most cells. The reesterification of MAGs is represented in the monoacylglycerol pathway. The respective enzymes are highlighted in red. GPAT: glycerol-phosphate acyltransferase; AGPAT: acyl-glycerol-phosphate acyltransferase; PAP: phosphatidic acid phosphohydrolase; MGAT: monoacylglycerol acyltransferase; DGAT: diacylglycerol acyltransferase.

FFA for TAG storage are typically provided through dietary fat uptake. Upon nutritional uptake, lipids are partially degraded through lingual lipases and pancreatic lipases to MAGs and FFA. Lipid resorption in the intestine is ensured through the aggregation of micelles through the action of bile acids. To enable the transport of water insoluble lipid components to ectopic tissues, the residues need to get re-esterified to TAGs and packed up in specialized lipoproteins for further distribution. These lipoproteins can be divided according to the composition of the transported lipid species and the ratio between lipid and protein content in chylomicrons, very low-density lipoproteins (VLDL), low-density lipoproteins (LDL), and high-density lipoproteins (HDL) [20]. Chylomicrons and VLDL are the main lipoproteins for TAG transport and are predominantly responsible for the distribution from the

intestine and the liver, respectively. Mucosa cells in the intestine are responsible for the synthesis of immature chylomicrons that are associated with the apolipoprotein B₄₈. These precursors associate with TAGs and other lipid species and further lipoproteins to mature chylomicrons that are distributed through the lymph. The production of VLDL is comparable to chylomicrons with B₁₀₀ as the predominant apolipoprotein [20]. HDL and LDL are mainly responsible for the transport of cholesterol and cholesterol ester and are important for the regulation of cholesterol biosynthesis.

A specialized extracellular lipase, lipoprotein lipase (LPL) is responsible for the breakdown of TAGs within chylomicrons or VLDL to enable the uptake of FFA in the cells. Fatty acids are able to pass the cell membrane either through passive diffusion or active transport through specialized fatty acid transporter proteins. Adipocytes express two important families of fatty acid transporters: fatty acid transport protein (FATP) and fatty acid translocase (FAT or CD36) [20].

Besides the nutritional uptake, cells are capable of *de novo* lipogenesis, hence the synthesis of fatty acids from non-lipid sources. This event likely occurs upon fasting or the consumption of carbohydrate rich diets. *De novo* synthesis of FAs is catalyzed by a multienzyme complex, the fatty acid synthase (FASN). FASN is able to catalyze the synthesis of FAs up to sixteen carbon atoms, hence the main product of lipogenesis is the saturated FA palmitate (16:0). Further processing steps, including elongation and the introduction of double bonds, are carried out by specialized enzymes, elongases and desaturases, respectively. The activity of synthesizing FA from carbohydrate sources underlies rigorous regulation and is dependent on the dietary status, the composition of the incorporated nutrients and transcriptional regulation. SREBP1c, an insulin dependent transcription factor, plays a central role in the regulation process. Upon insulin stimulation, SREBP1c is activated, causing an increase in the transcription of lipogenic genes, including FASN and ACC [20].

TAG synthesis is catalyzed by two enzymes of the DGAT family, DGAT1 and DGAT2. *In vitro* studies suggest that cells with the single deletion of either DGAT1 or DGAT2 are capable of normal TAG synthesis and storage [22]. However, the deletion of both enzymes is associated with severe dysregulation in TAG metabolism as cells cannot build LDs anymore [22]. *In vivo* studies accounted DGAT2 as the main enzyme responsible for TAG synthesis rather than DAGT1, as animals with DGAT2 KO exhibited massive reduction in TAG levels, skin barrier abnormalities, and died shortly after birth [23].

Intracellular Lipolysis

FFA are stored in the form of TAGs within LDs in adipocytes. Lipolysis describes the breakdown of TAGs, hence the release of FFAs along with the glycerol backbone. Three enzymes are mainly involved in the breakdown of TAGs: Adipose triglyceride lipase (ATGL), hormone-sensitive lipase (HSL), and monoacylglycerol lipase (MGL). These three enzymes show the highest affinity to catalyze the first, second, and third step of intracellular lipolysis, respectively. A schematic overview of the lipolytic process is illustrated in **Figure 4**.

(CE), and retinyl esters (RE) and is therefore involved in various pathways including TAG breakdown and steroid metabolism. HSL is encoded by LIPE and is located on chromosome 19. It is expressed in minor amounts in various tissues and cells like cardiac and skeletal muscle, testis as well as pancreatic β - cells and macrophages [35]. However, WAT and BAT depots show the highest expression of HSL [35]. Two isoforms of HSL are encoded by the LIPE gene, which are generated by the usage of alternative translational start codons. The long form is expressed in steroidogenic tissues such as testis and is responsible mainly for CE hydrolyses. The short form is prenominal expressed in adipocytes, where it is involved in intracellular lipolysis to release NEFA along with glycerol [36].

According to their respective function, HSL structure can be divided into three domains: an N-terminal domain for enzyme dimerization and lipid binding, an C-terminal domain containing the catalytic triad (Ser₄₂₄, Asp₆₉₃, and His₇₂₃) and a regulatory region of the protein containing the phosphorylation sites of HSL [35]. HSL activity underlies rigorous regulation. The activity is primarily increased through phosphorylation and the translocation from the cytosol to bind perilipin 1 (PLIN 1) at LDs. This process occurs in an cAMP dependent manner with catecholamines stimulating and insulin inhibiting the activation of HSL.

The systemic deletion of HSL in mice causes DAG accumulation in various tissues including AT depots, cardiac and skeletal muscle and testis resulting in sterility of male mice [37]. Furthermore, these animals are resistant to diet induced obesity with reduced WAT but increased BAT weight [38], display AT inflammation and inhomogeneous distribution of adipocyte size [39]. In contrast, mice heterozygous for HSL deletion (HSL +/-) show normal development of body weight and AT depots, an improvement of systemic and AT insulin sensitivity as well as changes in metabolic substrate usage to favor glucose over FA metabolism [39].

The adipocyte specific deletion of HSL under the control of the aP2 promoter but not the liver specific deletion was associated with the development of hepatic steatosis [40]. The knockout of adipocyte HSL was also found to increase macrophage infiltration along with an increase of inflammatory markers and the development of systemic insulin resistance with age [40]. Furthermore, HSL is associated with the activation of PPAR γ , as it might provide ligands for binding. Humans bearing mutations in the encoding LIPE gene were found to have an increased risk for type 2 diabetes accompanied with dyslipidemia and hepatic steatosis [41]. Therefore, HSL is involved in fundamental metabolic pathways to maintain AT and non-AT function.

The last step of lipolysis is catalyzed through MGL. The 33 kDa protein shows no hydrolytic activity against TAGs or DAGs but is involved in the cannabinoid metabolism through degrading 2-arachidonoyl glycerol providing endogenous ligands for cannabinoid receptor binding. Animal studies with global MGL knockout mice revealed that hydrolytic activity in AT was partially compensated through HSL activity of these animals. Furthermore, KO mice were associated with improved glucose metabolism and insulin sensitivity, indicating an important role in systemic metabolism [42].

Regulation of Intracellular Lipolysis

The process of lipolysis underlies rigorous regulation through hormones and signaling molecules and is dependent on the dietary status of the individual. Under basal conditions, HSL is inactive and predominantly located in the cytosol. The LD surface is associated with PLIN1, acting as barrier to prevent the uncontrolled breakdown of lipid stores. In addition, PLIN1 is responsible for the binding of CGI-58, which upon binding causes to increase ATGL activity [12].

The deprivation of nutrients stimulates the activation of lipid breakdown through the release of catecholamines and glucocorticoids acting through β -adrenergic receptors to increase cellular cAMP levels. The circulation reaction of AMP is catalyzed through adenylate cyclase (AC). Elevated cAMP levels activate protein kinase A (PKA), an enzyme from the family of serine/threonine kinases, responsible for the phosphorylation of various lipolytic proteins including PLIN1 and HSL (Ser^{559/660}) [3]. The phosphorylation of PLIN1 causes the dissociation from the LD to enhance the access for lipases as well as the release of CGI-58 to promote the hydrolytic activity of ATGL [25]. The lipolytic activity of HSL is increased through the translocation of the enzyme from the cytosol to the LDs upon phosphorylation (**Figure 5**).

Lipolytic activity is suppressed through insulin, which is secreted from beta cells in the postprandial state. Upon binding to its respective receptor, the insulin receptor (IR), it triggers a signaling cascade leading to a degradation of cAMP and thereby inhibiting the phosphorylation of HSL and PLIN1. The binding of insulin to the IR is followed by a conformational change within its subunits, causing the autophosphorylation at multiple sites of the receptor. Further signaling transduction includes the phosphorylation of insulin receptor substrate (IRS), which in turn increases the activity of phosphoinositol kinase 3 (PIK3). PIK3 is involved in the phosphorylation of specific phospholipids, leading to the formation of phosphatidylinositol-3,4,5-triphosphate (PIP3), which acts as a docking site for a protein named PIP3-dependent kinase (PDK1), an upstream activator of protein kinase B (AKT). AKT is involved in the regulation of different metabolic processing, including the stimulation of GLUT4 to enhance glucose uptake. In terms of lipolysis, AKT activates phosphodiesterase 3b (PDE3b), which catalyzed the hydrolysis of cAMP [43]. In addition to the AKT dependent pathway, insulin was found to reduce the expression levels of ATGL through an mTORC1 mediated pathway [44].

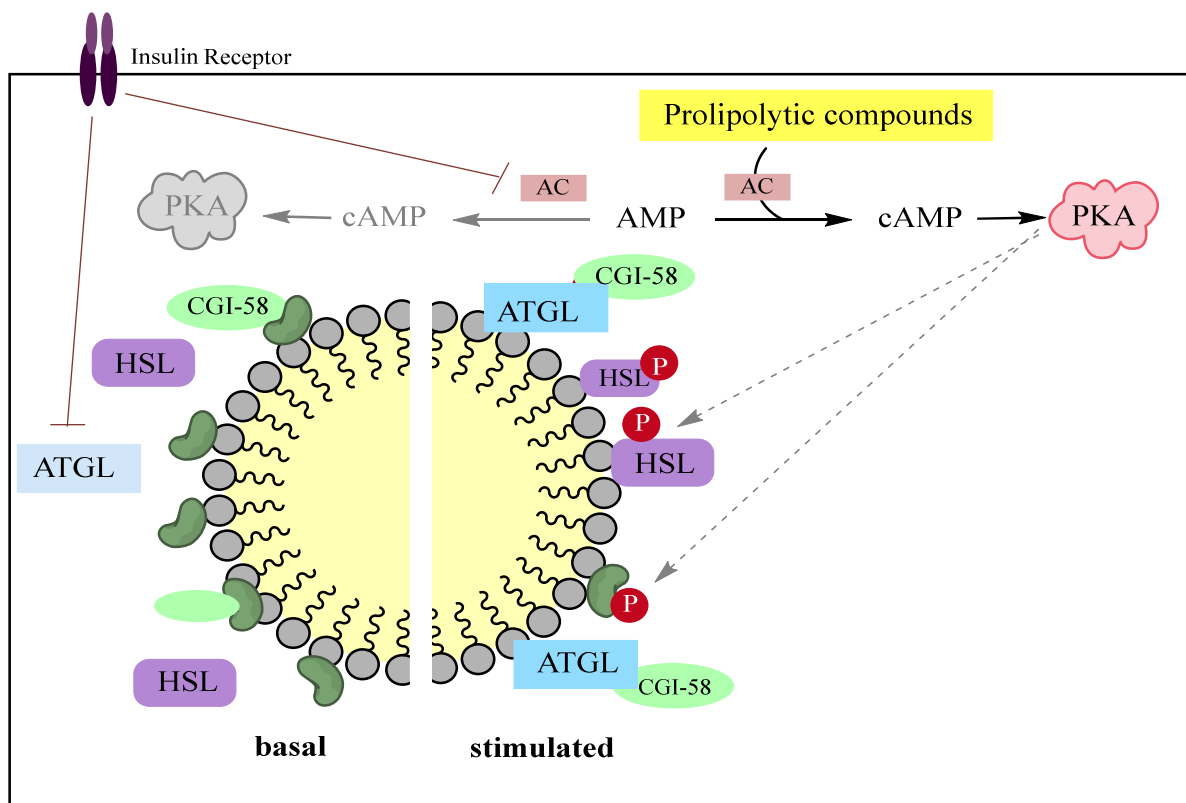


Figure 5: Regulation of Intracellular Lipolysis. Under basal conditions the lipid droplet is associated with PLIN1 (dark green) to prevent untargeted lipolysis. β -adrenergic stimulation through catecholamines increases cAMP levels within the cells causing the activation of PKA, which in turn phosphorylates HSL (violet) and PLIN1. Upon phosphorylation, PLIN1 dissociates from the lipid droplet surface and as well releases CGI-58 causing its binding to ATGL. The phosphorylation of HSL causes the translocation of the enzyme from the cytosol to the lipid droplet surface. Together, these events are responsible for the stimulated increase in lipolysis. Insulin acts as inhibitor of lipolysis to promote lipid storage through a decrease in cAMP levels and inhibition of ATGL (blue) expression. ATGL: adipose triglyceride lipase; CGI-58: comparative gene identification 58; HSL: hormone-sensitive lipase; PLIN1: perilipin 1; AMP: adenosine monophosphate; cAMP: cyclic adenosine monophosphate; PKA: protein kinase A; AC: adenylate cyclase

Glucose Metabolism

Nutritional carbohydrates provide an important glucose source for the body. The monosaccharide represents a central role in energy supply, especially for cells that are not capable of metabolizing lipids. For example, erythrocytes are solely dependent on energy supply through glucose metabolism, as they are lacking mitochondria for beta oxidation.

The glucose concentration in the blood needs to stay within a narrow range to provide proper energy supply especially for the brain. Therefore, blood glucose levels are strictly regulated, commonly through the interaction of the peptide hormones insulin and glucagon. The liver is considered as the major organ in glucose homeostasis as it regulates blood glucose concentration by storing excessive glucose in form of glycogen and producing as well as releasing glucose via gluconeogenesis and glycogen degradation. In the postprandial state, the concentration of circulating glucose increases and needs to be further processed. The uptake of glucose into the cells is mainly promoted through facilitated diffusion carried out by specialized protein transporters, the family of glucose transporters (GLUT) [20].

Adipocytes accomplish glucose uptake predominantly through the glucose transporter 4 (GLUT4), which is responsible for the insulin dependent uptake of glucose. The pancreatic peptide hormone insulin is secreted in the postprandial state to promote the uptake and storage of glucose through the induction of a signaling pathway resulting in an increase in the translocation of GLUT4 from the cytosol and the fusion with the plasma membrane [20].

The uptake of glucose is followed by the conversion to glucose-6-phosphate (G6P), which is the origin for further metabolic processing, including glycogen synthesis and glucose breakdown. The phosphorylation is catalyzed through hexokinase 2, which is regulated through G6P concentration *via* negative feedback reaction [20]. Glycolysis describes the breakdown of glucose resulting in the production of pyruvate and energy. Downstream metabolites of glycolysis are introduced in other metabolic pathways such as lipogenesis. Therefore, glucose and lipid metabolism are closely associated. An overview on adipocyte metabolism and the interaction between glucose and lipid metabolism is illustrated in **Figure 6**.

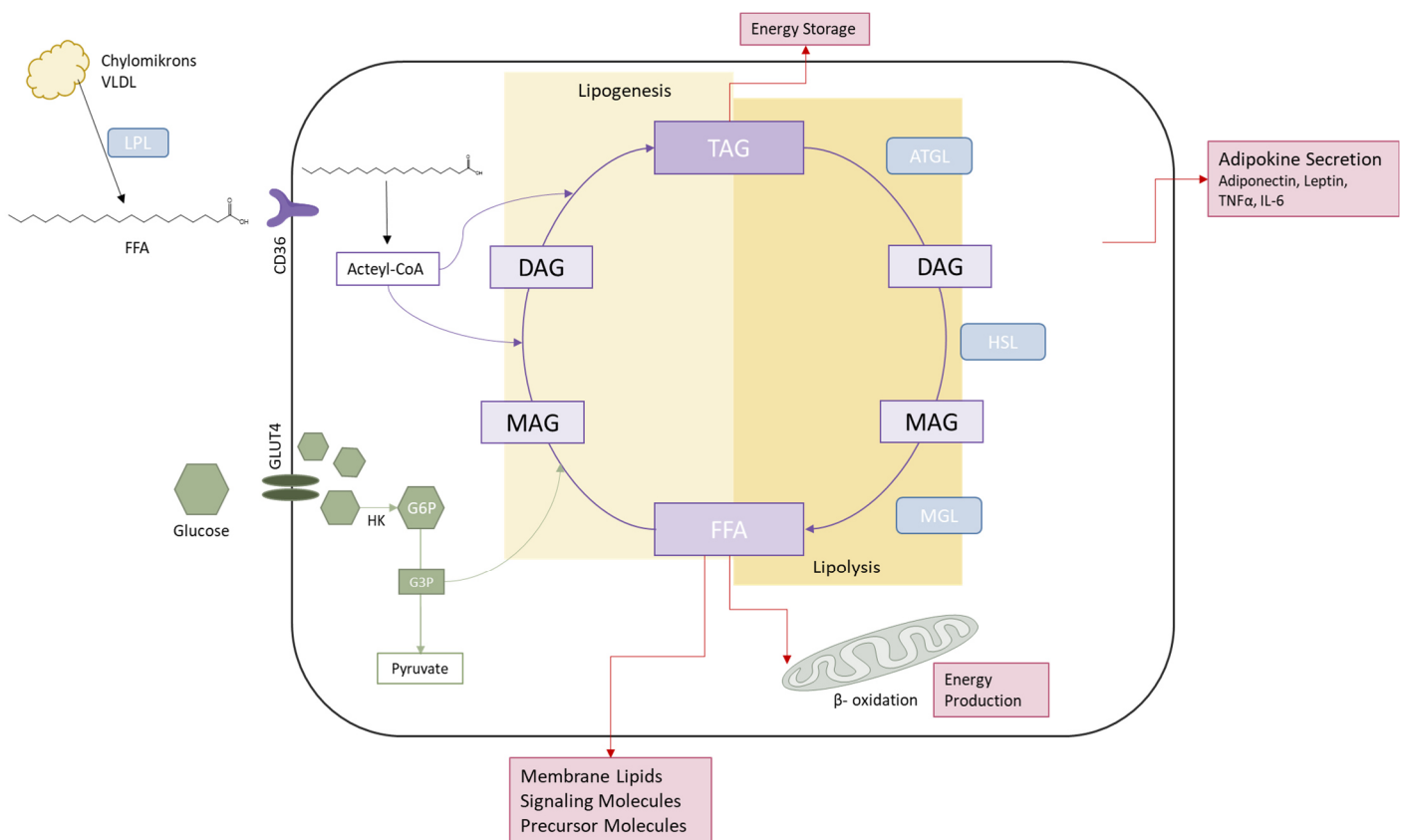


Figure 6: Schematic Overview on Adipocyte Metabolism. Triacylglycerol (TAG) stores are built in times of nutritional surplus and are hydrolyzed upon nutritional demand. TAG are transported in chylomicrons or very low-density lipoprotein (VLDL) and cleaved through lipoprotein lipase (LPL) before entering in form of free fatty acids (FFA) the cell through fatty acid transporters, e.g. CD36. FFA are either introduced to β -oxidation in the mitochondria or used for TAG synthesis, as membrane components, signaling molecules or precursors for further metabolic processing. Glucose is taken up by specialized transporters (GLUT4) and converted to glucose-6-phosphate (G6P). Glucose-3-phosphate (G3P), a downstream metabolite during glycolysis is introduced as backbone for TAG synthesis. Adipocytes are involved in the synthesis and secretion on adipokines that are involved in major metabolic processes, including systemic energy homeostasis and inflammation.

1.4 Adipokine Secretion

AT is not only involved in the whole-body energy supply but also plays an undisputable role in the production and secretion of various proteins, endocrine hormones, cytokines, and growth factors. Therefore, AT is involved in systemic processes including hunger and satiety, energy expenditure, glucose and lipid metabolism as well as immunity [45]. Important cytokines and proteins released from adipocytes include adiponectin, leptin, tumor necrosis factor α (TNF α), and IL-6. In addition, adipocytes secrete enzymes that are involved in steroid metabolism and proteins from the renin-angiotensin-aldosterone-system (RAAS) [5], [45].

The secretion pattern of the AT depot is closely related to its location and is also connected with the health status of the individual. For example, obesity is associated with an unbalanced relation in the secretion of pro- and anti-inflammatory adipokines [45].

Adiponectin is a small peptide (28 kDa) secreted by adipocytes and released into the plasma, where it is present as trimeric, hexameric or higher complex [45]. Dysregulations in adiponectin secretion are closely associated with obesity and the development of diabetes, where circulating levels of adiponectin are reduced. Mice with the systemic deletion of adiponectin show dysregulations in lipid metabolism and the development of severe insulin resistance [46]. Furthermore, high levels of adiponectin were found to have positive effects on the development of inflammation and atherosclerosis [5].

Another small peptide (16 kDa) secreted from adipocytes is leptin, which is encoded by the *obese* gene. Leptin is a known anorexigenic peptide, which is involved in the regulation of hunger and energy expenditure and due to structural similarities to cytokines in immune response [45] [46]. Leptin binds to its receptors, the leptin receptors (ObR), that are expressed in various tissues including the hypothalamus, where it is known to act as appetite suppressant. The secretion of leptin correlates with nutritional status, AT mass, and circadian rhythm [5], [47].

1.5 The Aim of the Thesis

The field of lipid metabolism is under intense research activity as it provides novel insights in systemic metabolism and the development of diseases. While ATGL-mediated lipolysis has been studied excessively within the last years, the contribution of adipocyte specific HSL to the development of metabolic diseases is still controversial. The aim of this master thesis is to enlighten the role of adipocyte specific HSL to adipocyte function on cellular and organismal level including its consequences on systemic energy, glucose, and lipid homeostasis *in vivo*.

The specific aims of this study were

- to determine the impact of HSL loss on adipocyte differentiation and adipose function in primary (pre)adipocytes *in vitro*
- to characterize the AT phenotype including AT function and inflammation of mice lacking HSL in adipocytes depending on age (young vs aged mice)
- to determine the consequences of adipocyte specific HSL loss to systemic lipid and glucose homeostasis *in vivo*

Therefore, we used a mouse model with the specific deletion of HSL in adipocytes, the AHKO mice. These mice express Cre recombinase under control of the mouse adiponectin (Adipoq) promoter along with a LoxP flanked (floxed) HSL gene resulting in the specific deletion of HSL in mature adipocytes of white and brown AT, but not macrophages.

2. Materials

2.1 Plastic and Hardware

Plastic ware including plates (6-well, 12-well) and 10 cm petri dishes as well as standard tubes of different size and PCR tubes (0.2 ml) were purchased from Greiner Bio One (Germany). Serological pipettes (5 ml, 10 ml, and 25 ml) were purchased from Corning Inc. (USA).

Plates and plastic films for quantitative PCR analysis were obtained from Applied Biosystems (Thermo Fisher Scientific; USA) or Biorad (United Kingdom). Sterile filter tips (20 μ l, 300 μ l, and 1250 μ l) were purchased from Biotix, Inc (USA).

2.2 Chemicals

If not other stated, chemicals used for all experiments were purchased from Sigma Aldrich, (St. Louis, USA), Merck (Whitehouse Station, USA), Thermo Fischer Scientific (Waltham, Massachusetts), Bio-Rad Laboratories (Vienna, Austria), Abcam Plc. (Cambridge, Great Britain), and Karl Roth (Karlsruhe, Germany).

2.3 Equipment

Centrifuge 5415 R	Eppendorf	Real-Time PCR System StepOnePlus	Thermo Fischer Scientific
Centrifuge GS-6	Beckman	SDS chambers Mighty Small II	Hoefer
ChemiDoc™ Touch Imaging System	BioRad	Spectrophotometer Nanodrop ND-100	PeQlab
Electrophoresis Power Supply- EPS600	Pharmacia Biotech Inc.	Thermo Cycler C1000TM	Biorad
Julabo waterbath	Seelbach-Germany	Thermomixer	Eppendorf
Liquid Scintillation Analyzer	Packard	Transfer chamber Mighty small TE22 transphor unit	Hoefer
Microplate Reader Multiskan FC	Thermo Fischer Scientific	Ultraturrax IKAR T10 Homogenizer Work center	IKA

2.4 Buffer and Solutions

Cell Culture, Protein, and RNA Isolation				
Collagenase D Solution			PBS (10X)	pH 7.4
Collagenase D	30 mg		KCl	27 mM
HEPES (0.5 M)	600 µl		NaCl	1.37 mM
CaCl ₂ (2.5 M)	25.2 µl		Na ₂ HPO ₄	43 mM
BSA (20% in ddH ₂ O)	500 µl		KH ₂ PO ₄	14 mM
PBS	20 ml			
5 ml per mouse and tissue depot				
			Protease Inhibitor	1000x
			Leupeptin	20 mg
DEPC water			Antipain	2 mg
DEPC	0.1%		Pepstain	1 mg
distilled water, autoclaved			in 1 ml DMSO	
Depletion Buffer			Protein Lysis Buffer	
NaCl	40 mM		SDS	0.1%
MgSO ₄	1.2 mM		NaOH	0.3 M
KCl	4.7 mM			
CaCl ₂	2 mM		TAE Buffer	pH 7.2
			Tris-HCl	40 mM
Erythrocyte Lysis Buffer			EDTA	50 mM
NH ₄ Cl	154 mM		Acetic Acid	7%
KHCO ₃	10 mM			
EDTA	0.1 mM		Transport Buffer	
			NaCl	40 mM
HSL Buffer	pH 7.0		MgSO ₄	1.2 mM
Sucrose	0.25 mM		KCl	4.7 mM
EDTA	0.5 M		CaCl ₂	2 mM
DTT	1 mM		KH ₂ PO ₄	1.2 mM
Protease Inhibitor	0.1%		Deoxyglucose	0.1 mM
Phosphatase Inhibitor			³ H Deoxyglucose	0.5 µCi/well
Oleic Acid (complexed)				
Oleic Acid	4 mM			
BSA (fatty acid free)	3.4 mM			

SDS Gel electrophoresis and Western Blot				
Acrylamid	30%		Stripping Buffer	pH 6.7
			Tris-HCl	62.5 M
APS	10% in H ₂ O		SDS	2%
			Mercaptoethanol	140 µl/20 ml
Blocking Solution				
milk powder	10% in TST			

CAPS Buffer (Transfer Buffer)	10x		Tris-Glycin Buffer	10x
CAPS	10 mM		Tris	200 mM
Methanol	10%		Glycine	1.6 M
			SDS	0.83%
Coomassie Destaining Solution				
Acetic Acid	8%		TST (10x)	pH 7.4
Methanol	30%		Tris-HCl	500 mM
			NaCl	1.5 M
Coomassie Staining Solution			Tween20	1%
Ethanol	50%			
Acetic Acid	6%		Upper Buffer (4x)	pH 6.8
Coomassie-brilliant blue R250	0.25%		Tris-HCl	0.5 M
Lower Buffer (4x)	pH 8.8			
Tris-HCl	1.5 M			
SDS Loading Dye (4x)	pH 6.8			
Tris-HCl	200 mM			
Dithiothreitol	400 mM			
SDS	8%			
Glycerin	40%			
Bromophenol blue	0.05%			

ORO Staining and TLC Analysis				
Fixing solution			TLC Eluent	
Formalin	4% in PBS		Hexane	70%
			Diethylether	29%
ORO Stock Solution			Acetic acid	1%
ORO powder	1 mg/ml H ₂ O			
			TLC Substrate	
ORO Working Solution			Copper Sulphate	10%
ORO stock solution	3:2 in dH ₂ O		Phosphoric acid	10%
Incubation	10 min at RT			
Filtration	0.45 µm			

2.5 Media

Standard Media			Maintenance Media	
DMEM/F-12 + GlutaMAX™	Thermo Fisher Scientific		Standard Media	
FCS	10%		Insulin	5 µg/ml
PenStrep	1%			
Primocin	0.2%			
Differentiation Media			Low Glucose Media	
Standard Media			DMEM Low glucose (1g/l)	Thermo Fisher Scientific
IBMX	0.5 mM			
Dexamethasone	1 µM			
Insulin	5 µg/ml			
Rosiglitazone	1 µM			

2.6 Kits

Quantitative Polymerase Chain Reaction				
<i>Previous Kit</i>			<i>New Kit</i>	
Perfecta DNase 1 Kit	Quantabio		DNase 1 (RNase free)	New England Biolabs
High capacity cDNA reverse transcription kit	Thermo Fisher		LunaScript RT SuperMix Kit	New England Biolabs
Determination of Free Fatty Acids and Glycerol				
NEFA Determination	Fujifilm		Glycerol Determination	Sigma-Aldrich
NEFA-HR R1a			Free Glycerol Reagent	
NEFA-HR R2a			Glycerol Standard	2.5 mg/ml
NEFA Standard	1 mM			
BCA Protein Determination				
Pierce BCA Protein Assay	Thermo Scientific			

2.7 Western Blot Analysis

Protein standard for SDS gel electrophoresis

Color Prestained Protein Standard, Broad Range (New England Biolabs)

ECL reagents (BioRad)

Clarity™ Western Peroxide Reagent

Clarity™ Western Luminol/Enhancer Reagent

Detection

Bio Rad Chemidoc System

Separating gel (5 gels)	10% acrylamide	16.4 ml ddH ₂ O, 10 ml 4x lower buffer, 13.2 ml 30% acrylamide, 400 µl 10% SDS, 36 µl TEMED, 108 µl 10% APS
Stacking gel	4.5% acrylamide	0.59 ml ddH ₂ O, 0.25 ml 4x upper buffer, 0.15 ml 30% acrylamide, 10 µl 10% SDS, 1.3 µl TEMED, 6 µl 10% APS, 0.5% blue dye

Primary and Secondary Antibodies

Table 1: Primary and Secondary Antibodies used for Western Blot Analysis.

Primary Antibodies					
Protein	Dilution	Species	Company	Order number	kDa
Anti-total AKT	1:1,000; in 5% milk	Rabbit	Cell signaling	C67E7	60
Anti-pAKT (Ser473)	1:1,000; in 5% milk	Rabbit	Cell signaling	9271S	60
Anti-ATGL	1:1,000; in 5% milk	Rabbit	Cell signaling	C.S.#2138S	54
Anti-CGI-58	1:1,000; in 5% milk	Mouse	Abnova	H00051099-M01	58
Anti-GAPDH	1:20,000; in 5% milk	Rabbit	Cell signaling	C.S.#2118S	37
Anti-HSL	1:1,000; in 5% milk	Rabbit	Abcam	C.S.#4107S	80
Anti-Plin1	1:1,000; in 5% milk	Rabbit	Sigma	P1998	62
Secondary Antibodies					
Anti-Rabbit	1:10,000; in 2% milk	-	Vector Laboratories	PI-1000	-
Anti-Mouse	1:10,000; in 2% milk	-	GE Healthcare UK	NA931V	-

2.8 Real Time PCR Primer

Table 2: Primer Sequences for Gene Expression Analysis using RT-PCR.

Gene	Direction	Sequence (5'-3')
Adiponectin	forward	CCGGGACTCTACTACTTCTCTT
	reverse	TTCCTGATACTGGTCGTAGGT
Cd11c	forward	CAGTGACCCCGATCACTCTT
	reverse	CACCACCAGGGTCTTCAAGT
Cd36	forward	GAACCTATTGAAGGCTTACATCC
	reverse	CCCAGTCACTTGTGTTTTGAAC
C/ebp α	forward	CAAGAACAGCAACGAGTACCG
	reverse	GTCACTGGTCAACTCCAGCAC
Cyclophilin	forward	TTCCAGGATTCTGTGCCAG
	reverse	CCATCCAGCCATTCAGTCTT
Dgat2	forward	TTCCTGGCATAAAGGCCCTATT
	reverse	AGTCTATGGTGTCTCGGTTGAC
F4/80	forward	GGATGTACAGATGGGGGATG
	reverse	CATAAGCTGGGCAAGTGGTA
Fabp4	forward	AAGGTGAAGAGCATCATAACCCT
	reverse	TCACGCCTTTCATAACACATTCC
Fasn	forward	TCCTGGAACGAGAACACGATCT
	reverse	GAGACGTGTCACTCCTGGACTTG
Hsl	forward	GCT GGG CTG TCA AGC ACT GT
	reverse	GTA ACT GGG TAG GCT GCC AT
Il-6	forward	GAGGATACCACTCCCAACAGACC
	reverse	AAGTGCATCATCGTTGTTCATACA
Pepck	forward	CATATGCTGATCCTGGGCATAAC
	reverse	CAAACCTCATCCAGGCAATGTC
Ppar γ 2	forward	CCAGAGCATGGTGCCTTCGCT
	reverse	CAGCAACCATTGGGTCAG
Srebp1c	forward	GTTACTCGAGCCTGCCTTCAGG
	reverse	CAAGCTTTGGACCTGGGTGTG

3. Methods

3.1 Western Blot Analysis

Protein Isolation from Adipose Tissues (total homogenate)

Adipose tissue depots were homogenized in HSL buffer containing protease (leupeptin, antipain, pepstain; Sigma-Aldrich) and phosphatase (PhosStop; Roche) inhibitors using the ultra turrax homogenizing system. Remaining fat was filtered through a cell strainer (100 μm ; VWR) and proteins were precipitated with acetone (10x) over night at -20°C . The samples were centrifuged for 30 min at 14,000 rpm and 4°C . Afterwards, the pellet was washed in chloroform to remove remaining lipid contaminations and then resuspended either in HSL buffer for protein determination or 1x SDS loading dye for western blot analysis.

Protein Isolation from Cells

Cells grown in 6-well plates were directly harvested in 500 μl 1x SDS loading buffer and 12 μl of the respective sample were applied to the SDS gel.

Determination of Protein Concentration

Protein concentration was determined using BCA analysis kit. A standard curve was prepared with bovine serum albumin (BSA) between 0 and 2,000 $\mu\text{g}/\text{ml}$. Lysates of cells or tissues were analyzed either directly or after acetone precipitation. The BCA reagents were combined according to manufacturer's instructions. Measurements were performed in 96 well plates using 100 μl of BCA reagent for 10 μl of sample. After incubation for 30 min at 37°C , absorbance was measured at 560 nm.

SDS-Gel electrophoresis and Membrane Transfer

Proteins were segregated by their molecular weight using sodium dodecyl sulphate-polyacrylamide gel electrophoresis (SDS-PAGE). Therefore, gels (10% acrylamide) were prepared as stated above. Proteins (10 μg) from adipose tissue homogenates were diluted in SDS loading dye after acetone precipitation. Cell culture samples were harvested in SDS loading dye and 12 μl were directly loaded to the gel. Protein segregation was performed at 20 mA amperage in SDS chambers (Mighty Small II; Hoefer) under constant water cooling in Tris-Glycine buffer.

For further analysis proteins were spotted to a PVDF membrane in a transfer chamber (Mighty small TE22 transphor unit; Hoefer) with CAPS buffer at 200 mA for 70 min under constant water cooling.

Membranes were incubated in milk solution (10% milk in TST) for at least one hour at RT or overnight at 4°C to block unspecific binding of the antibodies. Primary antibodies were applied to the membrane and incubated either at RT for two hours (GAPDH) or overnight at 4°C. Antibodies were diluted in milk solution according to manufacturer's statement as summarized above in **Table 1**. Afterwards, membranes were washed with TST (3x 10 min) and then incubated with the secondary antibody (1:10,000 in 2% milk) for at least one hour at RT. Membranes were washed again (3x 10 min) and characteristic bands were identified by detection of chemiluminescence of horseradish peroxidase, coupled to secondary antibody. Therefore, ECL reagents (Clarity™ Western ECL Substrate, BioRad) were used and signals were detected on the ChemiDoc™ Touch imaging system (Biorad). Between the analyses using different primary antibodies, the membrane was stripped at 54°C for 10 min in stripping buffer. Quantification of the respective signals was performed using the Image Lab software.

3.2 RNA Isolation and cDNA synthesis

RNA was isolated from subcutaneous (SCAT) and perigonadal (PGAT) adipose tissue from both AHKO and wildtype mice. The tissues were homogenized in 500 µl Trizol® (BioRad) reagent on ice using ultra turrax homogenizing system and RNA was precipitated according to manufacturer's statement. An additional step of centrifugation (10 min, 15,000xg, 4°C) was introduced to remove excessive lipid content. Primary cells were washed once with PBS and were directly harvested in 500 µl Trizol per 6 well and further processed to manufacturer's statement. The isolated RNA was dissolved in water (Fresenius) and RNA concentration was determined by photo spectroscopy using NanoDrop® Spectrophotometer (Peqlab Biotechnology). Samples were diluted properly to a final RNA concentration of 200 ng/µl with water.

Residual genomic DNA was removed by DNase I digestion following manufacturer's protocol. The transcription to cDNA was performed with 1 µg of RNA using reverse transcription kit.

3.3 Quantitative Real-Time PCR (RT-PCR)

Differences in mRNA gene expression were determined using quantitative real-time polymerase chain reaction (RT-PCR). For analysis, the DNA intercalating fluorescent dye SYBR green (Biorad) was used and the signal was quantified relative to the housekeeping gene cyclophilin. The prior reverse transcribed cDNA was diluted 1:25 in water (Fresenius) and 4 µl (1 µg cDNA) were used for analysis. For each reaction, 10 µl SYBR and 1 µl forward and reverse primer were used. Primers were diluted according to the manufacturer's information and equal concentration of the respective primer pair was verified on agarose gels (1% agarose). Primer sequences of the analyzed genes are summarized (**Table 2**). Analysis was performed in the StepOnePlus Real time PCR system (Applied Biosystems) with the following temperature program (**Table 3**).

Table 3: Temperature Program used for RT-PCR analysis.

time	2 min	10 min	15 sec	1 min
Temperature [°C]	50	95	95	60
Repeat 40x				

3.4 Animals

Mice with the specific deletion of HSL in adipocytes (AHKO) were generated by crossing mice with a loxP flanked HSL gene (floxed) with mice expressing Cre recombinase under the control of the mouse Adiponectin promoter [37]. Mice were backcrossed to a C57BL/6J background for at least ten generations. Animals were housed in a pathogen free environment with an 14:10 h light:dark cycle at 25°C. Unless otherwise stated, mice had ad libitum access to water and food. All animals for this study were males and fed a high fat diet (HFD; 42 kJ% fat; E15744, Ssniff Spezialdiäten GmbH).

3.5 Determination of Plasma Lipid Parameters

Plasma was obtained by centrifugation of whole blood for 10 min at 3,000 rpm and 4°C

NEFA determination

Plasma levels of non-esterified fatty acids (NEFAs) were determined using an enzymatic colorimetric method assay (FujiFilm). Therefore, 5 µl of plasma were incubated with 100 µl of the R1A solution for 10 min at 37°C. Afterwards, 50 µl of solution R2A were added and incubated for 10 min at 37°C. A standard curve was prepared using the NEFA standard (1 mM). Absorption was measured at 560 nm.

Glycerol determination

Plasma glycerol level was determined using the free glycerol kit (Sigma). A standard curve was prepared using glycerol standard (2 mg/ml) from Sigma. Plasma (5 µl) and standard solutions were incubated with 150 µl of glycerol reagent for 10 min at 37°C and the absorption was measured at 560 nm.

3.6 Primary Cell Culture

For all cell culture experiments, including isolation of stromal vascular fraction, cell cultivation, and differentiation of preadipocytes, complete media (DMEM/F-12, GlutaMAX™; ThermoFisher Scientific) containing 10% fetal bovine serum (Fisher Scientific-Gibco™), 1% Penicillin/Streptomycin (Fisher Scientific-Gibco™), and 0.2% Primocin (Lonza Cologne) was used. Cell culture experiments were

performed under sterile conditions in a laminar flow workbench. Cells were grown in an incubator at 37°C, 7% CO₂, and 95% humidity. Upon reaching confluency (70-80%), cells were harvested by trypsinization (0.5% Trypsin Fisher Scientific-Gibco™) and seeded in plates depending on the performed experiments.

Isolation of SVC

Stromal Vascular Fraction (SVF) was isolated from SCAT of both wildtype and AHKO mice. Mice were sacrificed by cervical dislocation and tissues were taken and dissected in PBS. The pieces were transferred into freshly prepared and sterile filtered collagenase D solution and incubated at 37°C for approx. 45 min at 110 rpm. Reaction was inactivated by adding complete media.

Undigested material was removed by filtration through a 100 µm cell strainer. Cells were pelleted (5 min, 600 g, RT;) and the supernatant was removed. Cells were resuspended in 1 ml erythrocyte lysis buffer and incubated for 2 min. The reaction was stopped by adding 10 ml complete media. The solution was filtered through a 45 µm cell strainer and the remaining cells were pelleted again, resuspended in 10 ml complete media, and seeded in 10 cm petri dishes. After reaching confluency, cells were harvested using trypsin, counted, and seeded according to the performed experiments. 30,000 cells per 6 well and 15,000 cells per 12 well.

Differentiation of Adipocytes

Adipocyte differentiation was initiated in 2 days post-confluent preadipocytes by changing normal complete media to differentiation media containing the proadipogenic reagents Dexamethasone (Sigma-Aldrich), IBMX (Sigma-Aldrich), Rosiglitazone and Insulin. Two days after administration, media was changed to maintenance medium containing insulin. The maintenance medium was changed every second day until successful differentiation (8-10 days).

For the experiments regarding differentiation capacity, no Rosiglitazone was added to the differentiation media.

3.7 Oil Red O Staining (ORO)

ORO working solution was prepared right before usage by diluting the stock solution in water (3:2) and filtering through a 25 µm filter. Cells were washed twice in PBS and fixed by adding formalin (4%) and incubating for 15 min at RT. Cells were washed twice with dH₂O and isopropanol (60%) and dried at RT. Working solution was added and the cells were incubated for 45 min at RT without shaking. Microscopical imaging was performed after washing with dH₂O. For photometric quantification of the ORO signal, the dye was extracted in isopropanol for 15 min at RT. Absorption of the sample was measured at 492 nm.

3.8 Thin Layer Chromatography

To investigate neutral lipid accumulation during differentiation of primary adipocytes, thin layer chromatography (TLC) was performed. Lipids were extracted from primary cells before initiating the differentiation process (day 0) and on day 2, 4, and 8 after differentiation using Hexane:Isopropanol (3:2) two times for 10 minutes. The organic solvent was dried under nitrogen steam and lipids were resuspended in Chloroform (100 μ l). The remaining proteins were lysed in SDS/NaOH (0.1%, 0.3 N) for protein determination using BCA. Lipid samples were spotted on TLC (TLC Silica gel 60 F₂₅₄ aluminium sheets; Merck) normalized to protein concentration and separated in Hexane:Diethylether:Acidic acid (70:29:1). Separated Lipids were visualized after administration of CuSO₄ in the oven (130°C) for 30 min.

3.9 Radioactive Assays

In Vitro Glucose Uptake

For glucose uptake experiments, primary cells were seeded in 12-well plates (15,000 cells/well). The uptake was performed using primary preadipocytes (before initiating adipogenesis) and adipocytes (10 days of differentiation). Maintenance media was changed to standard media (DMEM + P/S + FCS+ Primocin) without insulin the day before starting the experiment. Cells were incubated with depletion buffer including 2% BSA (fatty acid free; Sigma-Aldrich) for 20 min at 37°C. Media was changed to transport buffer containing both radioactive labelled (1 μ Ci/ml; Perkin Elmar) and "cold" 2-deoxyglucose (0.1 mM). To stimulate glucose uptake, insulin (10 μ g/ml) was added in both depletion and transport buffer. After incubation with transport buffer for 20 min at 37°C, media was discarded, and cells were lysed in 600 μ l SDS/NaOH (0.1%; 0.3 N) at RT. Cell lysates (500 μ l) were measured by liquid scintillation (Rotiszint® eco plus LSC Universal cocktail, Roth) in the beta counter (Packard). Protein concentration was determined using BCA analysis.

In Vitro Fatty Acid Uptake

Oleic Acid Uptake

For fatty acid uptake experiments, primary cells were seeded in 12-well plates (15,000 cells/well) and differentiated for 10 days. Primary adipocytes were incubated with low glucose medium containing oleic acid (400 μ M complexed with BSA) and radiolabeled ³H oleic acid (1 μ Ci/ml complexed with BSA; American Radiolabeled Chemicals) in the absence or presence of insulin (10 μ g/ml). The uptake was observed over 10 min. After incubation, cells were washed once with medium containing FCS (1%) to remove the remaining FA from the cell surface. Afterwards, cells were washed with PBS three times and lysed in 600 μ l SDS/NaOH (0.1%, 0.3 N) for four hours at RT. The intracellular uptake of FA was determined after two, five, and ten minutes, respectively. Cell lysates (500 μ l) were measured by liquid scintillation (Roth) in the beta counter (Packard). Protein concentration was determined using BCA analysis.

Bromo-Palmitate Uptake

Bromo-Palmitate (American Radiolabeled Chemicals; 0.1 μ Ci/ μ l) uptake into primary cells was observed after five minutes. Cells were incubated with depletion buffer for 20 min. Afterwards, low glucose medium containing 14 C-2-Bromo-Palmitate was applied to the cells. After incubation, cells were washed once with medium containing FCS (1%) to remove remaining FA from the cell surface. Afterwards, cells were washed with PBS three times and lysed in 600 μ l SDS/NaOH (0.1%, 0.3 N) for four hours at RT. Cell lysates (500 μ l) were measured by liquid scintillation (Roth) in the beta counter (Packard). Protein concentration was determined using BCA analysis.

In vivo Glucose and Bromo-Palmitate Uptake

The uptake of radiolabeled 3 H 2-deoxyglucose (Perkin Elmer; 1 μ Ci/ μ l) and 14 C Bromo-Palmitate (American Radiolabeled Chemicals; 0.1 μ Ci/ μ l) was performed within one experimental approach in 20-week-old AHKO and control mice on HFD. Mice were fasted for 6 hours before administering 3 H 2-deoxyglucose (10 μ Ci/mouse in 90 μ l saline) intraperitoneally. Five minutes later, Bromo-Palmitate (1 μ Ci/mouse in 90 μ l saline) was injected intravenously. Blood samples were taken 10 and 15 minutes after glucose administration. Afterwards, animals were sacrificed by cervical dislocation. After perfusion with PBS, tissues were taken and lysed in SDS/NaOH (0.1%; 0.3 N). Cell lysates (500 μ l) and blood (10 μ l) were measured by liquid scintillation (Roth) in the beta counter (Packard). Protein concentration was determined using BCA analysis.

In vivo Oleic Acid Uptake

The uptake of radiolabeled 3 H oleic acid was performed in 22-week-old AHKO and control mice on HFD. Mice were fasted overnight and 3 H-Triolein (2 μ Ci/mouse; American Radiolabeled Chemicals) was administered within an olive oil gavage (200 μ l). Thereby, 3 H-Triolein and olive oil were mixed using the bendelin sonicator. Two hours after the oral lipid bolus, animals were sacrificed by cervical dislocation. Blood was taken shortly before scarification. Tissues were taken after perfusion the animal with PBS and lysed in SDS/NaOH (0.1%; 0.3 N). Cell lysates (500 μ l) and blood (10 μ l) were measured by liquid scintillation (Roth) in the beta counter (Packard). Protein concentration was determined using BCA analysis.

3.10 Statistics

All results are shown as average values with the standard error of the mean (SEM). Significance was determined by two-tailed students t-test and marked regarding to the p-value with $p \leq 0.05 = *$, $p \leq 0.01 = **$, $p \leq 0.001 = ***$.

4. Results

Previous studies in mice revealed that unlike in ATGL deficient animals [24], the systemic deletion of HSL is not associated with the development of obesity, whether upon high caloric diet nor due to backcrossing to a genetically obese background [48][49]. However, deregulations in lipid metabolism, including the accumulation of DAG species within several tissues and the development of hepatic steatosis, were observed in HSL-KO mice [37][40]. In addition, the deletion of HSL was associated with reduced expression of PPAR γ targets genes which are predominantly involved in adipogenesis, lipid synthesis, and lipid uptake in AT of mice [48]. This suggests that HSL is, besides its important role in lipid breakdown, capable of providing substrates or precursor molecules for the activation of the transcription factor PPAR γ and thereby regulating systemic glucose and lipid metabolism [48]. Therefore, we evaluated the impact of adipocyte specific HSL deletion on AT phenotype and function *in vitro* and *in vivo*

4.1 Consequences of Adipocyte Specific HSL deletion *in vitro*

Adipocyte Differentiation

Adipocyte differentiation is the initial step to provide proper adipocyte function. To investigate whether adipocyte specific deletion of HSL had an impact on the adipocyte differentiation process, stromal vascular cells (SVC) were isolated from SCAT depots of AHKO and control mice, cultivated and differentiated by adding the pro-adipogenic reagents Dexamethasone, IBMX, and insulin. To investigate the ability of preadipocytes to induce the differentiation process, PPAR γ agonist rosiglitazone was not supplied to the cells. The differentiation progress was observed over 10 days and samples for RNA isolation and measurements of lipid content were taken every other day. Although it would have been of great interest to investigate adipocyte function of primary cells obtained from visceral AT depots, we could not establish a protocol to sufficiently isolate and cultivate primary cells from PGAT.

The adipocyte specific HSL knockout (AHKO) mouse model expresses Cre recombinase under the control of the adiponectin (*AdipoQ*) promoter. Therefore, the deletion of HSL is restricted to adipocytes and directly linked to the expression of adiponectin. Gene expression patterns in primary control cells showed a steadily increase in HSL mRNA expression from day two onward, reaching its maximum at day six. However, deletion of HSL in knockout cells occurred only in the late phase of adipocyte differentiation. A significant difference in HSL mRNA expression between control and knockout cells was detected from day four onward after differentiation initiation. This significant drop in HSL mRNA levels correlated with the expression pattern of adiponectin, which represents a key marker of the late phase of adipocyte differentiation and was found to be unaltered between control and knockout cells (**Figure 7**).

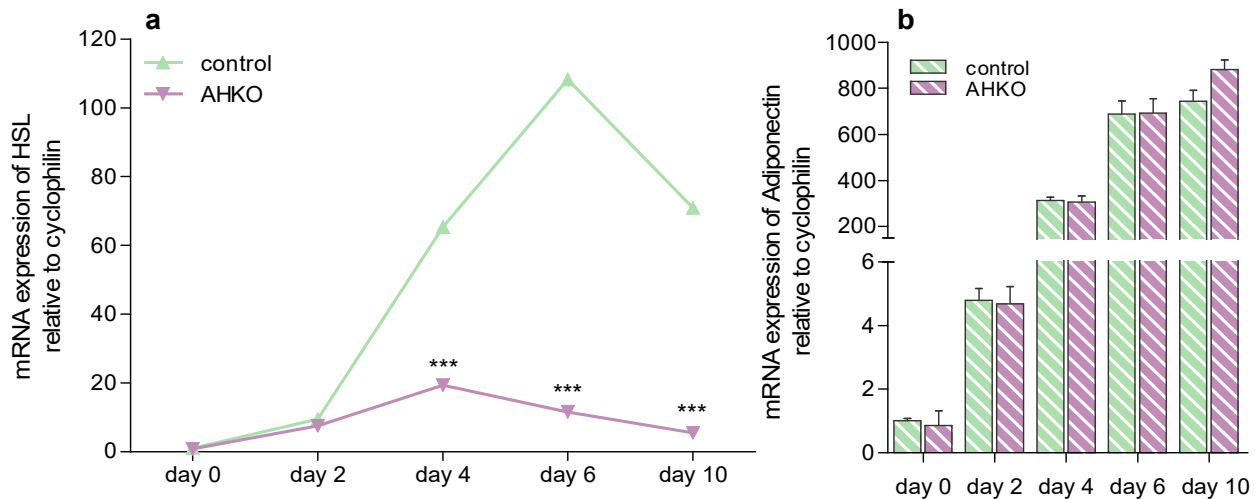


Figure 7: mRNA Expression Levels of HSL and Adiponectin in Primary Adipocytes during Adipogenesis. Cells were isolated from subcutaneous AT depots of AHKO and control mice. Differentiation was initiated 2 days after the cells reached confluency. The deletion of HSL is under the control of adiponectin promoter and occurred in the late phase of adipogenesis. a) mRNA levels of hormone sensitive lipase (HSL) and b) mRNA levels of adiponectin. Values represent the fold-change of the respective gene relative to cyclophilin reference gene by qPCR with endogenous gene expression in control preadipocytes (day 0) arbitrarily set to 1. Values are represented as average + SE. Significance between genotypes was determined by student's t-test ($p \leq 0.001 = ***$).

Adipogenesis is characterized by major changes of the expression pattern within precursor cells differentiating preadipocytes to mature adipocytes with distinct phenotype and functions. The interaction of several proteins and transcription factors is crucial to initiate and maintain the adipocyte differentiation process. Analysis of gene expression of regulatory transcription factors involved in adipogenesis, *Ppar γ 2*, *C/ebp1 α* and *Srebp1c*, did not reveal any differences between wildtype and knockout cells, demonstrating an adequate response to adipogenic stimulation and initiation of the differentiation process to mature adipocytes (**Figure 8**). Despite an initial downregulation of the expression level of *Ppar γ 2* in preadipocytes isolated from knockout animals, the expression was comparable to control cells after the initiation of adipogenesis. The expression levels of *Ppar γ 2*, which is considered as the main regulator of adipogenesis, was already significantly increased two days after the initiation of the differentiation process in control and knockout cells. *Ppar γ* is known to induce the expression of *C/ebp1 α* , which in turn gives positive feedback to stimulate *Ppar γ* expression [12]. Similar to *Ppar γ* expression, an increase in mRNA levels of *C/ebp1 α* was observed from day two onward. In contrast, *Srebp1c* was upregulated only in the late phase of adipogenesis. Although the induction of *C/ebp1 α* and *Srebp1c* expression were overall lower compared to *Ppar γ* , they were enough to maintain the differentiation process in primary cells.

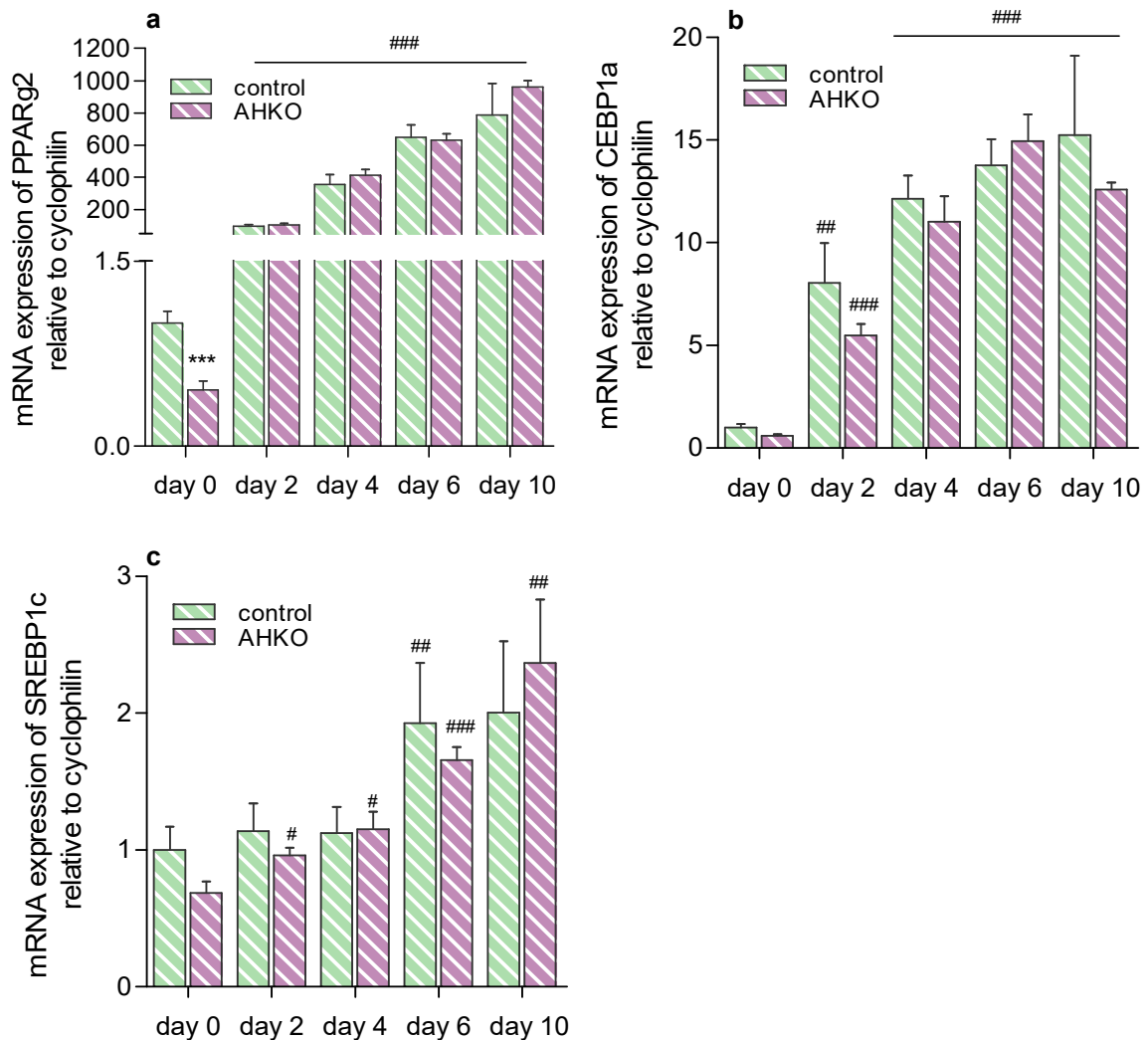


Figure 8: Differentiation Ability of Primary Adipocytes. Cells were isolated from subcutaneous AT depots of AHKO and control mice. Differentiation was initiated 2 days after the cells reached confluency. mRNA levels of the transcription factors *Pparγ2* (a), *C/ebp1α* (b) and *Srebp1c* (c) were not altered between control and knockout cells. The expression of these main regulators of adipogenesis are necessary to provide proper initiation of the differentiation process. Expression of *Pparγ2* and *C/ebp1α* were upregulated in the early phase of adipogenesis whereas mRNA levels of *Srebp1c* were increased only during the late phase. Values represent the fold-change of the respective gene relative to cyclophilin reference gene by qPCR with endogenous gene expression in control preadipocytes (day 0) arbitrarily set to 1. Values are represented as average + SE. Significance between genotypes was determined by student's t-test ($p \leq 0.001 = ***$).

In addition to the adipogenic gene expression pattern, the ability to generate LDs was not altered in cells lacking HSL compared to control cells, as total levels of neutral lipid content were unaltered between the cells. The accumulation of neutral lipids was visualized through staining of the cells using the azo dye Oil Red O (ORO) and quantified through photometric measurements of the extracted dye (**Figure 9 a+b**). Since ORO stains neutral lipids including TAG and CE, we evaluated lipid composition during adipogenesis using thin layer chromatography (**Figure 9c**). Preadipocytes were characterized through lacking TAGs, which steadily accumulated after the initiation of the differentiation process. In a similar way, accumulation of 1,2 DAG species was only observed in cells after eight days of

differentiation whereas the amount of 1,3 DAG species was not different during adipogenesis. Quantification of TAG accumulation during adipogenesis demonstrated comparable TAG levels between the genotypes with a tendency to be increased in KO cells at day eight. An accumulation of DAG species, like observed in other studies, was not detectable in primary KO cells.

An initial decrease in intracellular CE content was observed in the early phase of the differentiation in both control and KO cells. These data demonstrated that except for a minor increase of TAGs and 1,2-diaclyglycerol species in differentiated KO cells, lipid species were comparable between control and KO cells during different stages of adipocyte differentiation (**Figure 9c**).

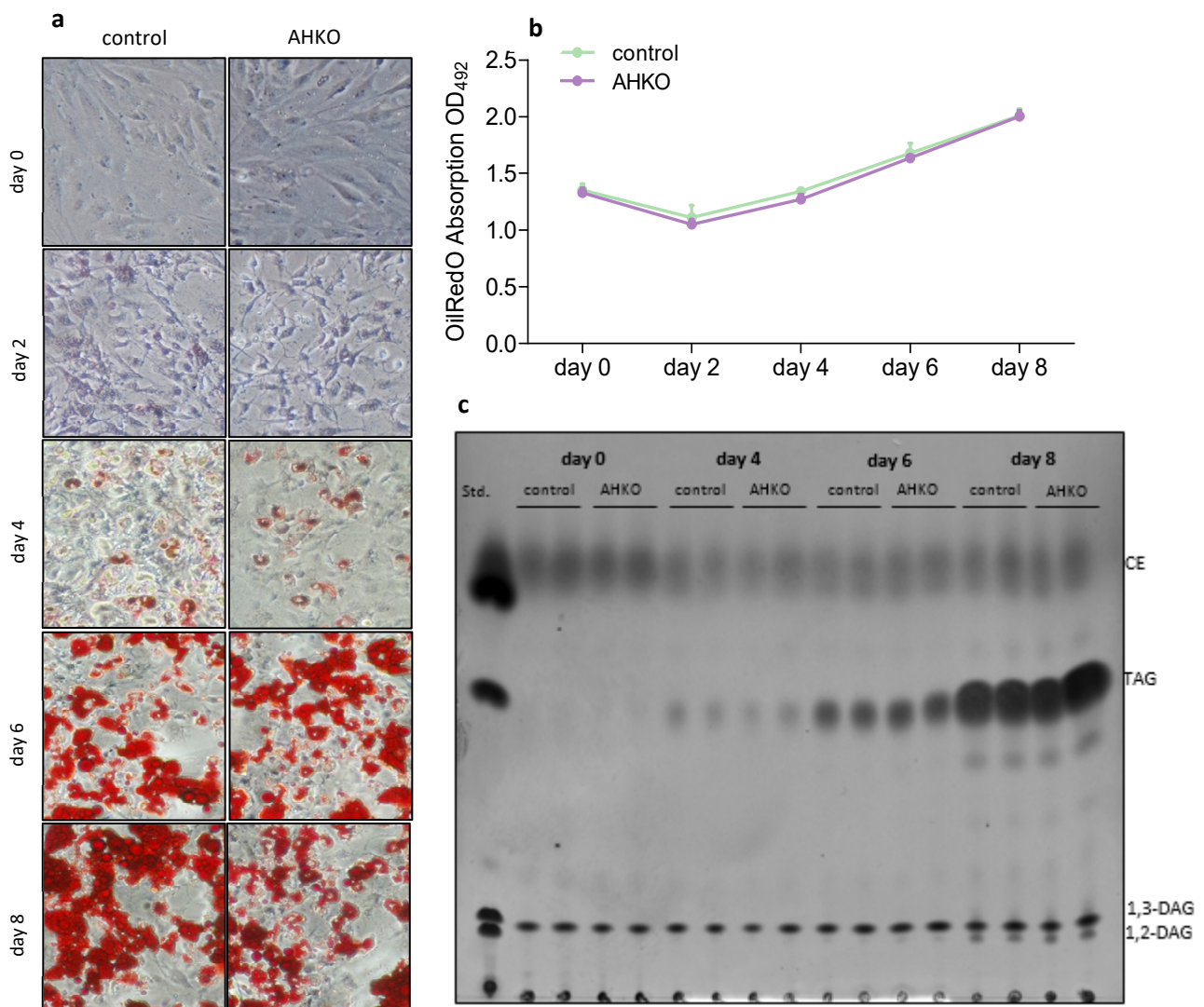


Figure 9: Analysis of Intracellular Neutral Lipid Content of Primary Cells during Adipogenesis. Cells were isolated from subcutaneous AT depots of AHKO and control mice. Differentiation was initiated 2 days after reaching confluency. Primary cells lacking HSL did not show impaired capacity of neutral lipid storage. a) Microscopic images of ORO stained primary cells during differentiation (day 0 - day 8). b) Photometric quantification of the extracted ORO dye to determine intracellular neutral lipid content. c) Lipid analysis of primary cells during differentiation using thin layer chromatogram. Values are represented as average + SE.

Adipocyte Function

Since primary adipocytes did not show differences in adipogenesis, indicated by similar accumulation of neutral lipids and expression of key adipogenic genes, we further investigated adipocyte function, including glucose and FA uptake in KO and control cells.

Glucose provides important molecules for energy production, such as pyruvate. The product of glycolysis is introduced in the citric cycle and gets further processed to generate ATP. In addition, intermediates of this process are utilized for TAG synthesis. Therefore, the uptake and metabolic processing of glucose is crucial for cell development and survival.

Measurements of mRNA levels showed that the expression of *Glut 4* was not altered in control and knockout preadipocytes. Adipocyte differentiation induced the expression of *Glut4*. However, mature adipocytes lacking HSL showed a significant increase in *Glut4* mRNA levels compared to control cells, suggesting improved glucose uptake in AHKO adipocytes (**Figure 10a**).

Glucose uptake using radiolabeled 2-deoxyglucose (2DG) was performed in primary cells before (preadipocytes) and after ten days of differentiation (adipocytes). Since insulin is responsible to enhance glucose uptake within the cells through binding to its respective receptor and the subsequent translocation of the glucose transporter GLUT4 to the plasma membrane, we performed the uptake under basal and insulin stimulated conditions. Determination of intracellular glucose uptake in preadipocytes revealed a reduced uptake in cells lacking HSL compared to control cells under basal, but not under insulin-stimulated conditions. Notably, glucose uptake was not induced upon insulin treatment, despite increased phosphorylation of AKT Ser⁴⁷³, indicating that the insulin signaling cascade was active in preadipocytes (**Figure 10b**). Although AHKO adipocytes exhibited higher *Glut 4* mRNA expression, mature adipocytes did not show significant differences in glucose uptake between the genotypes independent of insulin. However, and in contrast to preadipocytes, glucose uptake was induced upon insulin treatment in adipocytes (**Figure 10c**). These results indicate normal cellular function regarding glucose uptake and insulin signaling in HSL-deficient (pre)adipocyte *in vitro*.

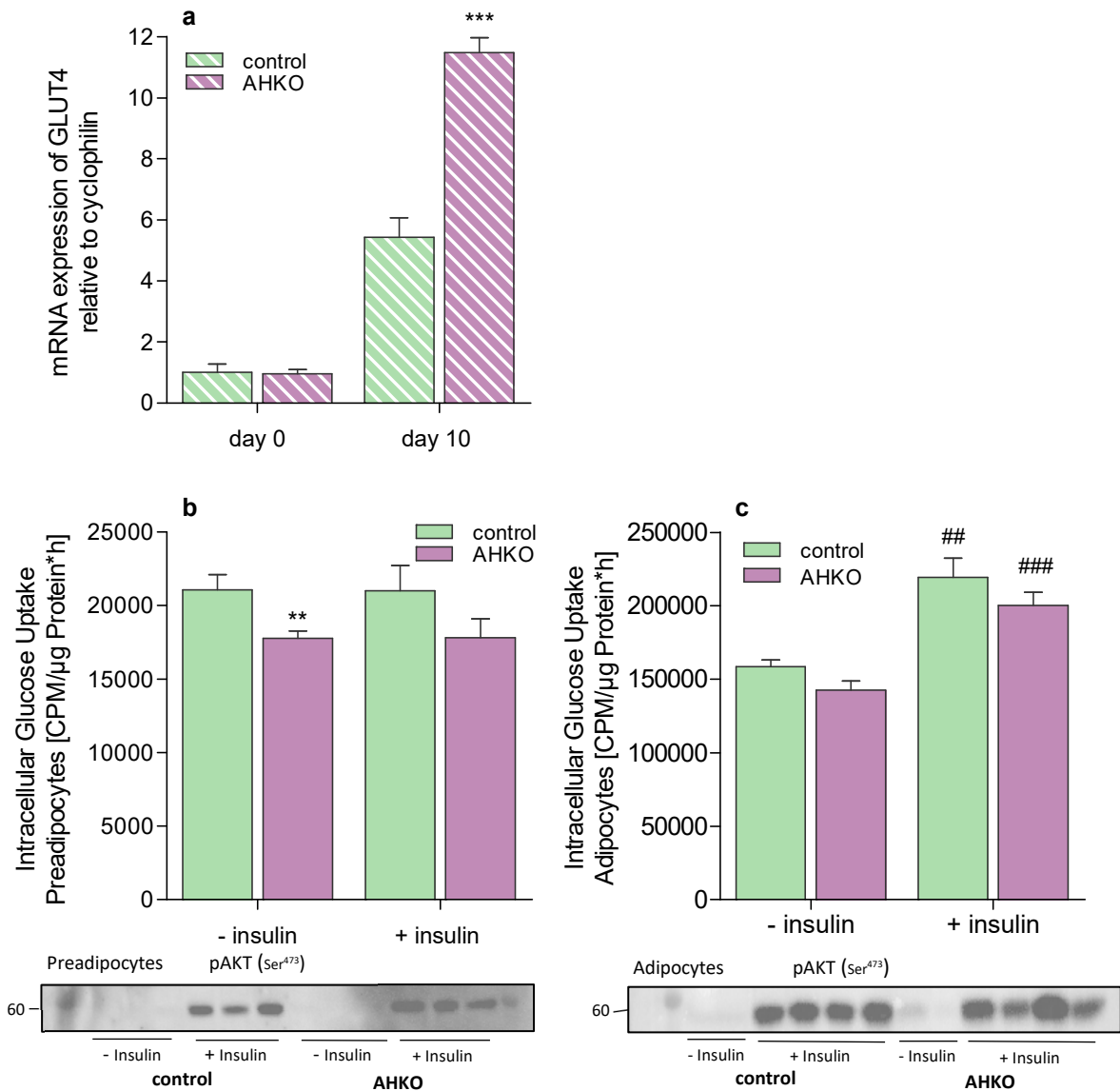


Figure 10: Intracellular Glucose Uptake in Primary Adipocytes and Reaction to Insulin Stimulation. Cells were isolated from subcutaneous AT depots of AHKO and control mice and differentiated for ten days to adipocytes. Glucose uptake was observed over 20 min using radiolabeled 2DG (0.5 μ Ci/well) as substrate. Preadipocytes lacking HSL showed decreased glucose uptake compared to control cells. Insulin treatment (10 μ g/ml) did not enhance the uptake rate in preadipocyte control and knockout cells. Glucose uptake in mature adipocytes was not altered between the genotypes but reacted to insulin stimulation with increasing rates of glucose uptake and phosphorylation of AKT Ser⁴⁷³. a) mRNA expression levels of Glut 4. Values represent the fold-change of the respective gene relative to cyclophilin reference gene by qPCR with endogenous gene expression in control preadipocytes (day 0) arbitrarily set to 1. b) Glucose uptake in preadipocytes. Insert: Western blot analysis of pAkt Ser⁴⁷³ in preadipocytes treated with or without insulin. c) Glucose uptake in adipocytes after ten days of differentiation. Insert: Western blot analysis of pAkt Ser⁴⁷³ in adipocytes treated with or without insulin. Values are represented as averages with the standard error of the mean. Significance was determined by student's t-test ($p \leq 0.01 = **$, $0.001 = ***$ between the phenotypes and $p \leq 0.01 = ##$, $0.001 = ###$ between basal and insulin stimulated uptake).

Besides proper uptake of glucose, adipocyte function is characterized by endogenous neutral lipid storage capacity. Therefore, the uptake of FFA along with esterification to TAGs built the fundamental requirements for adipocyte metabolism.

FA uptake was performed with radiolabeled ³H-oleic acid and ¹⁴C-Bromo-Palmitate, a FA which is not prone to be metabolized in differentiated adipocytes. The uptake of oleic acid was monitored over ten

minutes, evidently showing an increase of radioactivity within the cells over time. Despite a minor decrease in intracellular FA content in AHKO cells within the first two minutes, oleic acid uptake was not altered between control and AHKO adipocytes after 5 and 10 min (**Figure 11a**). Since insulin levels stimulate FA uptake and its esterification into lipids, we also measured the FA uptake in the presence or absence of insulin. Again, the uptake of Bromo-Palmitate was not different between control and AHKO adipocytes. However, insulin treatment did not affect FA uptake whether in knockout or control cells (**Figure 11b**). Together, these data indicate a normal uptake of FA in primary AHKO adipocytes *in vitro*.

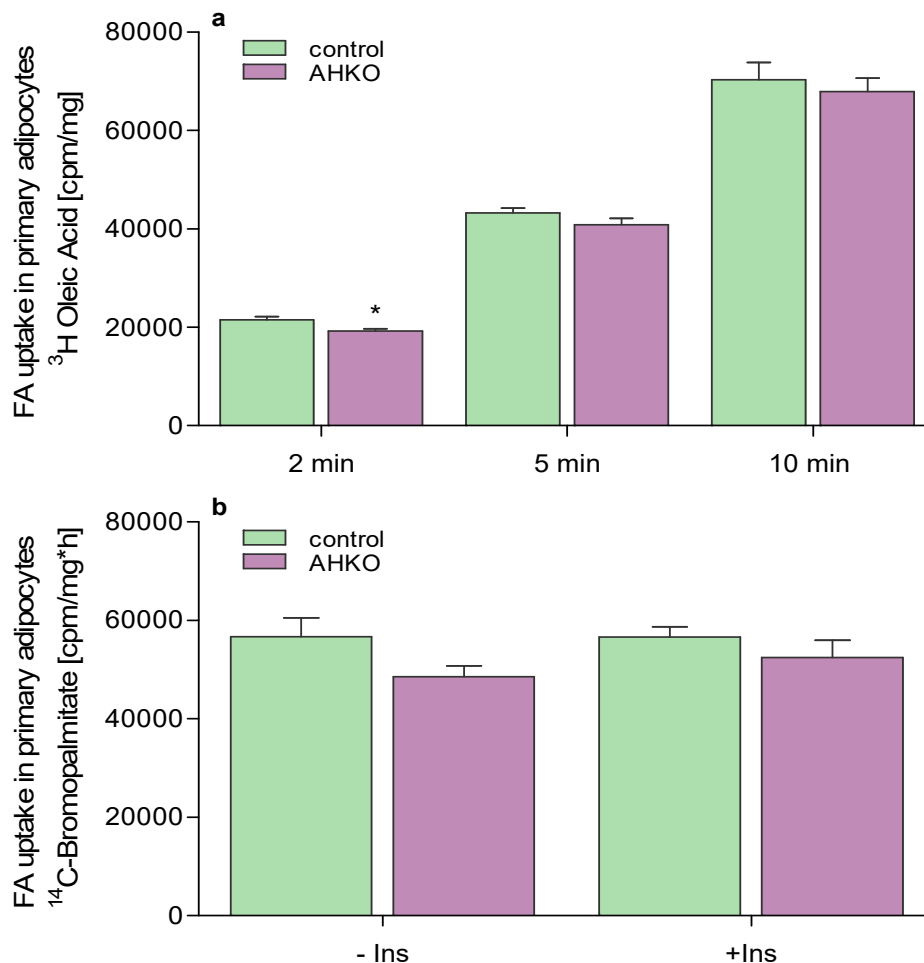


Figure 11: Fatty Acid Uptake using Different Substrates in Mature Adipocytes. Cells were isolated from subcutaneous AT depots of AHKO and control mice and differentiated for ten days to adipocytes. Adipocytes lacking HSL did not differ in fatty acid (FA) uptake. a) FA uptake of radiolabeled ($1 \mu\text{Ci/ml}$) ^3H -oleic acid after 2, 5 and 10 min and b) FA uptake of ^{14}C -Bromo-Palmitate ($0.5 \mu\text{Ci/ml}$) under basal and insulin ($10 \mu\text{g/ml}$) treated conditions after 5 min. Values are represented as averages with standard error of the mean. Significance was determined by student's t-test ($p \leq 0.05 = *$).

In conclusion, the loss of HSL in primary cells did not implicate dysfunction in adipocyte differentiation, neither in mRNA expression of adipogenic genes nor in accumulation of neutral lipids. Furthermore, no differences in glucose or FA uptake were observed between wildtype and HSL-KO cells. These results indicate sufficient adipocyte differentiation ability and function of AHKO (pre)adipocytes *in vitro*.

4.2 Consequences of Adipocyte Specific HSL Deletion *in vivo*

Since deletion of HSL in primary adipocytes did not change adipocyte function *in vitro*, we investigated the impact of adipocyte specific HSL loss on the AT phenotype and systemic metabolism in mice fed HFD *in vivo*.

AT Function and Health in AHKO mice

Body weight and fat mass of AHKO and control mice fed HFD was monitored over several weeks of age. Young mice showed similar body weight and total fat mass. However, with age body weight (22 weeks of age) and total fat mass (16 weeks of age) were significantly reduced in AHKO mice (**Figure 12a+b**). Accordingly, young mice showed no differences in PGAT and SCAT depots, whereas tissue weight of both AT depots was drastically reduced in aged AHKO mice (**Figure 12c**). The reduction in AT weight was more pronounced in PGAT (~80%) compared to SCAT (~40%).

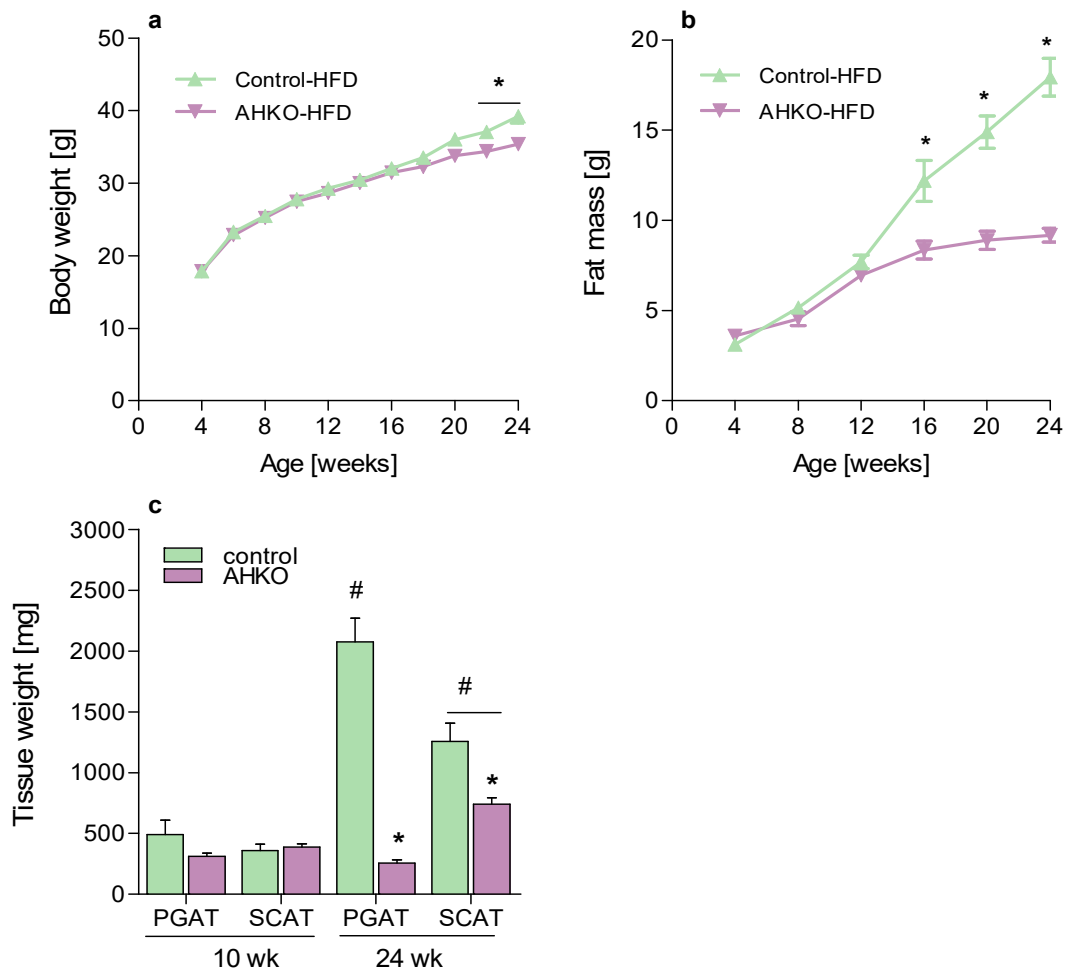


Figure 12: Body weight and fat mass of AHKO and Control Mice Upon High Fat Diet. Young AHKO mice showed similar body weight, fat mass, and AT weight compared to wildtype littermates. With age body weight was reduced and AT did not expand properly. This effect was especially pronounced in perigonadal AT. a) body weight, b) fat mass, and c) AT weight of perigonadal (PGAT) and subcutaneous AT (SCAT). Values are represented as averages with the standard error of the mean. Significance was determined by student's t-test ($p \leq 0.05$ = * for different phenotypes and $p \leq 0.05$ = # for differences in age).

According to the deletion of HSL in AT, AHKO mice exhibited impaired lipolytic activity. *Ad libitum* fed mice showed comparable plasma lipid parameters to control littermates. However, reduced plasma NEFA (-40%) and glycerol (-60%) levels were observed in AHKO mice under fasted conditions and independent of age (Figure 13).

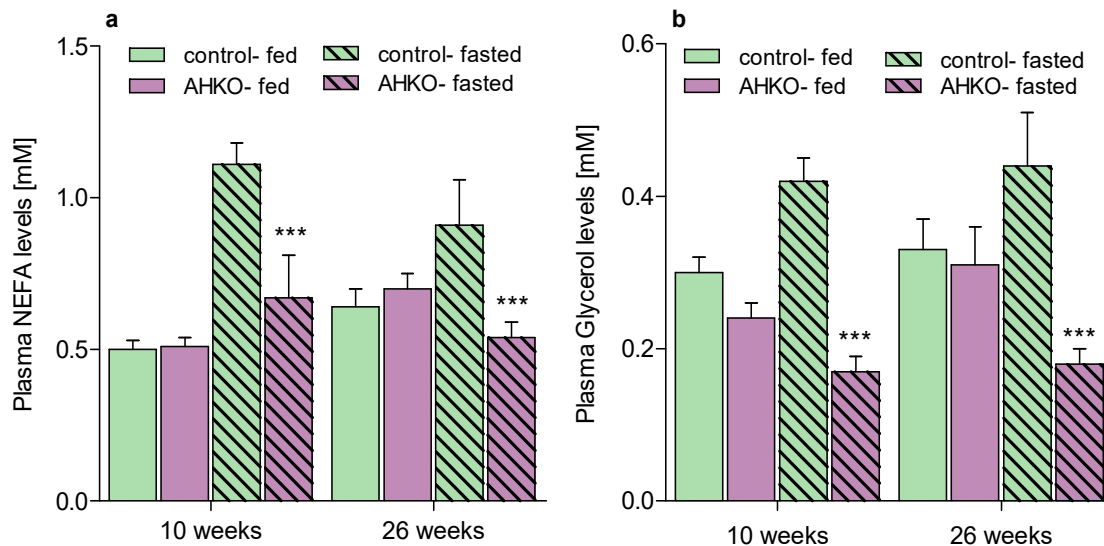


Figure 13: Plasma lipid Parameters of Control and AHKO Mice fed HFD. Both NEFA and glycerol levels were reduced in AHKO mice upon fasting. a) Plasma levels of non-esterified fatty acids (NEFA) and b) Plasma levels of free glycerol of 10 and 24-week-old mice in the *ad libitum* fed and 12h fasted state. Values are represented as average + SE. Significance between genotypes/different age was determined by student's t-test ($p \leq 0.05 = */\#$).

To evaluate whether HSL deletion had an impact on the entire lipolytic process, we determined expression levels of proteins involved in lipolysis. ATGL represents the main lipase in AT and is responsible to catalyze the first and rate-limiting step of TAG breakdown. The activity of ATGL is increased upon β -adrenergic stimulation through binding of its co-activator, CGI-58, increasing its lipolytic activity up to 20-fold [50].

Western blot analysis confirmed the deletion of HSL protein expression in WAT depots of young and aged AHKO mice (Figure 14a + Figure 15a). Protein levels of ATGL in control mice decreased with age leading to a reduction of ~50% in both AT depots in aged mice. However, ATGL protein expression was already significantly downregulated in both depots in young (-74% in PGAT, -40% in SCAT) and in aged (-90% in PGAT, -70% in SCAT) AHKO mice compared to control littermates (Figure 14b + Figure 15b). This reduction was accompanied with reduced levels of CGI-58. While CGI-58 expression was similar in young PGAT depots, the expression was downregulated (-70%) in SCAT from young AHKO mice. Nevertheless, both tissue depots showed a significant reduction in CGI-58 protein expression (-80%) upon 24 weeks of age (Figure 14c + Figure 15c).

PLIN 1 is located at the membrane of functional LDs to prevent untargeted lipolysis and is therefore associated with proper adipocyte function and health. Protein expression of Plin1 was not significantly altered between young and aged control mice on HFD despite an increased in AT mass. Interestingly, Plin1 levels were drastically reduced in AT depots of AHKO mice compared to control littermates (Figure 14d + Figure 15d)

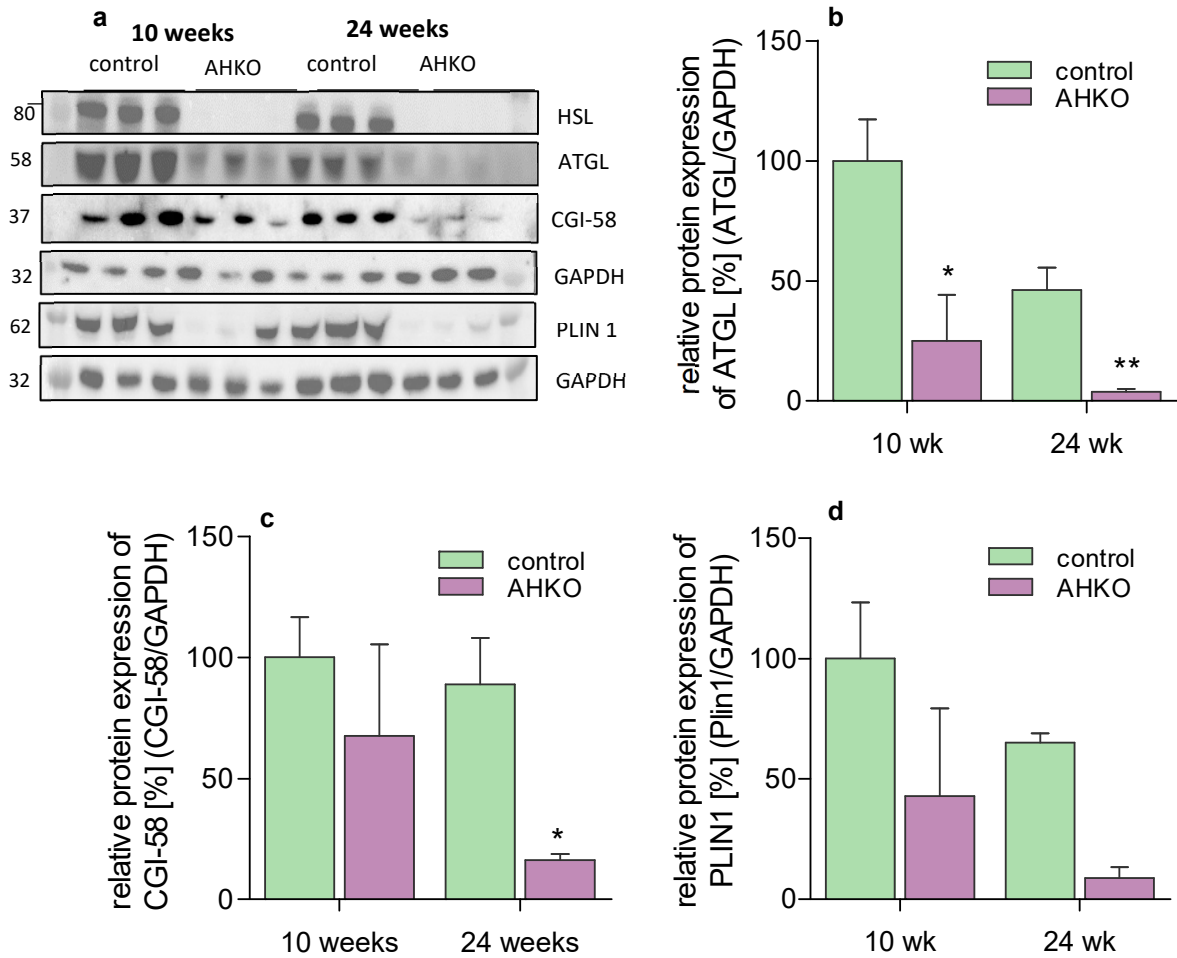


Figure 14: Expression of Lipolytic proteins in Perigonadal AT of Control and AHKO mice. Protein levels of ATGL and its co-activator CGI-58 were downregulated in young and old mice lacking HSL specifically in adipocytes. a) Western blot analysis (10 μ g protein) of respective proteins: HSL (80 kDa), ATGL (58 kDa), CGI-58 (37 kDa), PLIN1 (62 kDa). b-d) Quantification of the signal obtained from western blot. Values are normalized to GAPDH signal and are illustrated as average + SE. Significance was determined by student's t-test ($p \leq 0.05 = *$, $0.01 = **$).

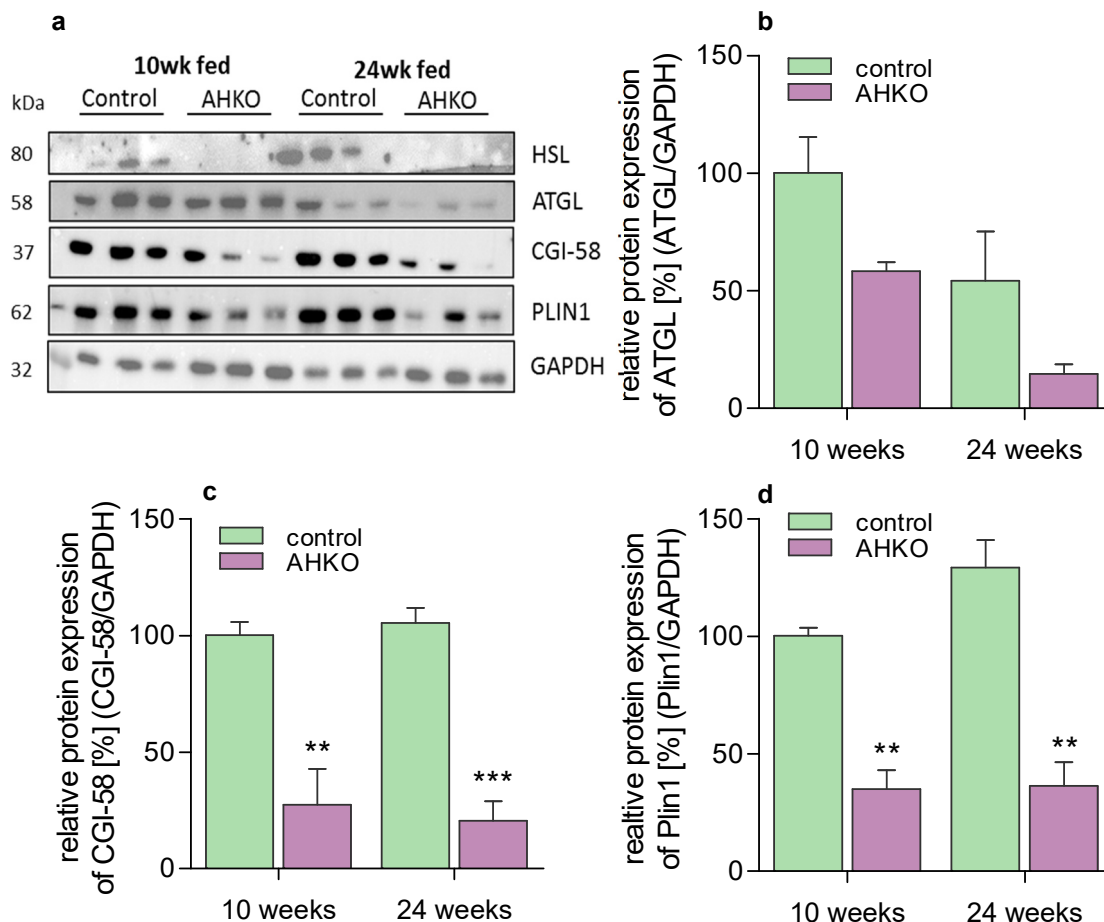


Figure 15: Expression of Lipolytic proteins in Subcutaneous AT of Control and AHKO mice. Protein levels of ATGL and its co-activator CGI-58 were downregulated in young and old mice lacking HSL specifically in adipocytes. a) Western blot analysis (10 μ g protein) of respective proteins: HSL (80 kDa), ATGL (58 kDa), CGI-58 (37 kDa), PLIN1 (62 kDa). b-d) Quantification of the signal obtained from western blot. Values are normalized to GAPDH signal and are illustrated as average + SE. Significance was determined by student's t-test ($p \leq 0.05$ = *, 0.01 = **).

AT represents a central organ for systemic homeostasis, not only through its role in energy supply but also as endocrine organ involved in the synthesis and release of various adipokines. Proper AT function is therefore closely associated with the prevention of metabolic diseases. Since AHKO mice exhibited reduced AT mass indicating dysregulation in AT metabolism, specific genes involved in fundamental AT function were investigated in young (10 weeks) and aged (24 weeks) mice fed HFD.

The expression of the main transcription factors responsible for the initiation of the differentiation process, *Ppar γ 2*, *C/ebp1a*, and *Srebp1c*, was similar between control and AHKO mice at 10 weeks of age. A downregulation of these genes was observed in both control and AHKO animals at 24 weeks of age. However, aged AHKO mice showed a significant reduction in the gene expression compared to control animals. This was true for both AT depots but was more pronounced in PGAT, where gene expression tended to decrease already in young mice (**Figure 16**). The downregulation of adipogenic genes indicates dysfunction in adipocyte development and may be associated with a reduced number of mature adipocytes in AT depots of AHKO mice.

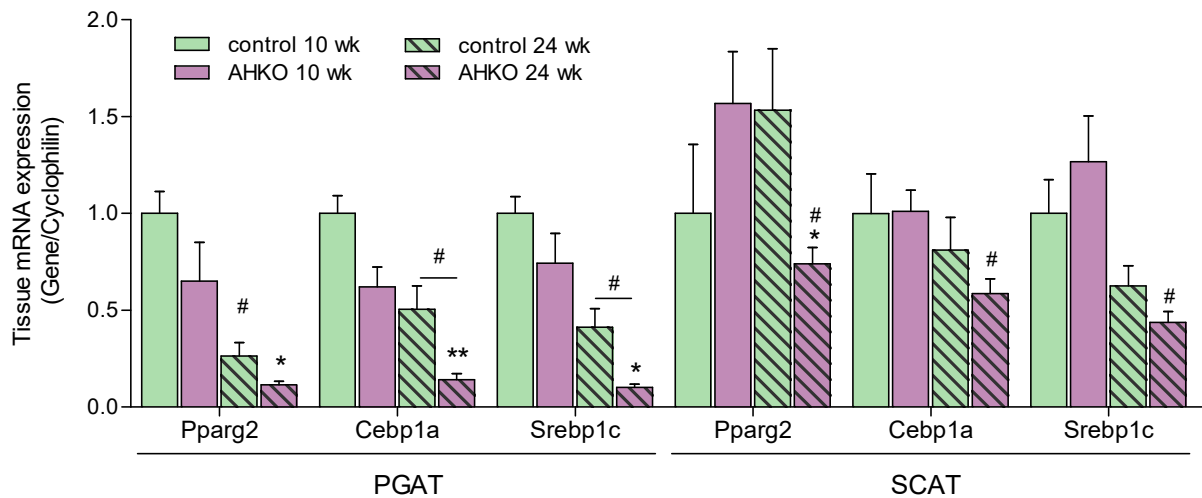


Figure 16: AT Expression of Adipogenic Genes in Young and Aged Mice. Main regulators of adipogenesis showed similar expression levels in AT depots of young mice whereas a significant downregulation was observed in aged AHKO mice. Values represent the fold-change of the respective gene relative to cyclophilin reference gene by qPCR with endogenous gene expression in ATs of control mice (10 weeks) arbitrarily set to 1. Values are represented as average + SE. Significance between genotypes/different age was determined by student's t-test ($p \leq 0.05 = *$, $0.01 = **$ / $p \leq 0.05 = \#$ for differences in age).

FA provide an important energy source. Especially in adipocytes, the uptake of FA is essential to build up energy reservoirs for times of nutritional demands. Investigations of the expression levels of fatty acid transporters revealed significant downregulation of both *Cd36* and *Fabp4* mRNA levels in PGAT of aged mice whereas the expression levels in SCAT were decreased however comparable to control littermates (**Figure 17a**).

The esterification of FFA to TAG is necessary to prevent the effect of lipotoxicity. DGAT2 is an important enzyme catalyzing the last step in TAG synthesis. Besides FA, the glycerol backbone is necessary for the re-esterification process to TAGs. The rate limiting enzyme in gluconeogenesis is PECK, providing glycerol-3-phosphate for TAG synthesis. Expression levels of *Dgat2* and *Pepck* were significantly downregulated in PGAT of young and aged AHKO mice. However, the expression of both genes was comparable in control and AHKO SCAT of young mice, but tended to decrease with age in AHKO mice (**Figure 17b**).

Besides FA uptake, cells are capable of synthesizing FA in times of nutritional surplus. The process of FA synthesis is mainly catalyzed by the multienzyme complex FASN. Gene expression of *Fasn* was decreased in PGAT, but unchanged in SCAT of young AHKO mice. Consistent to other genes involved in lipid synthesis, aged AHKO mice exhibited a downregulation of *Fasn* expression in both AT depots (**Figure 17b**).

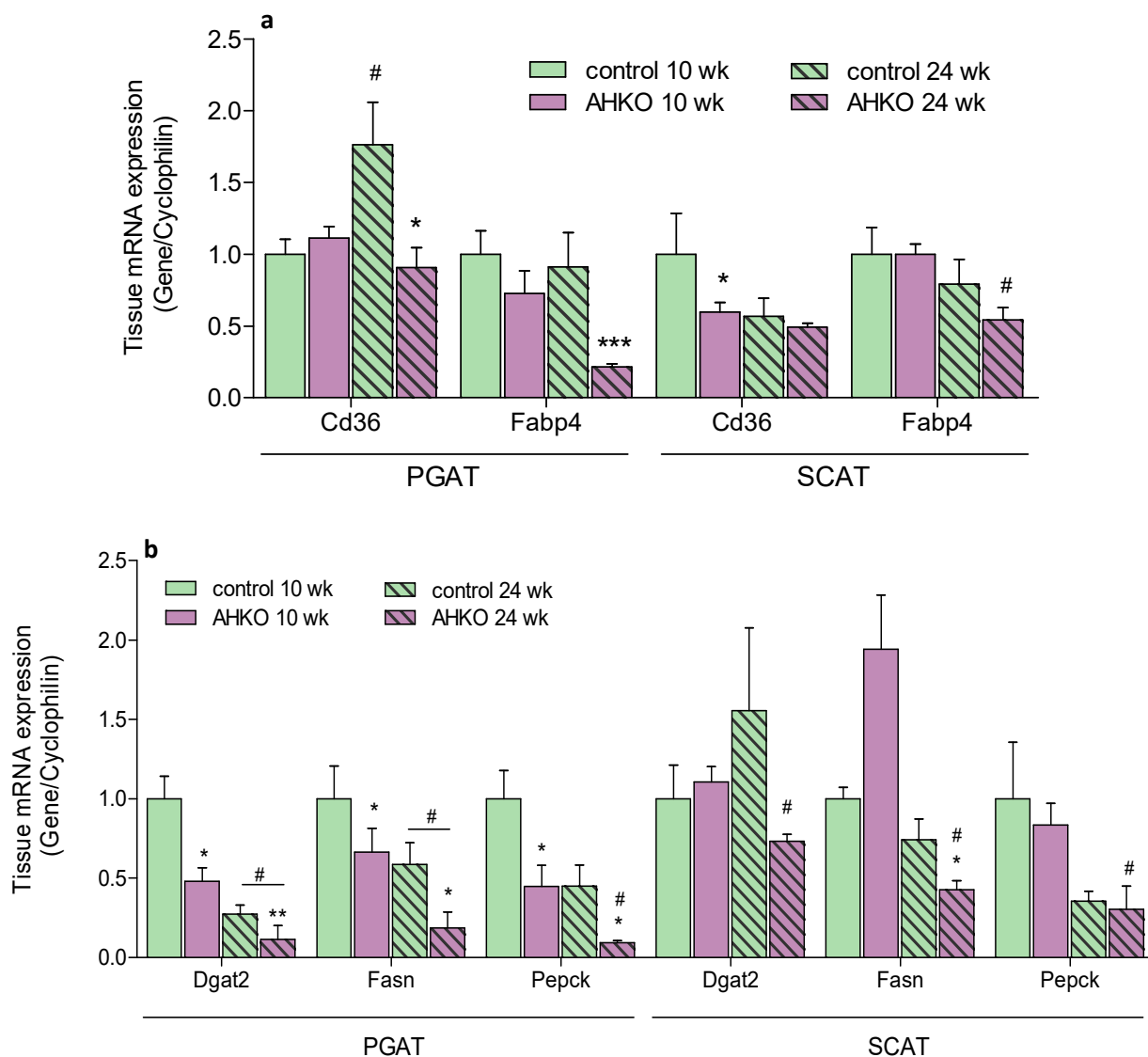


Figure 17: AT Expression of Fatty Acid Transporters and Genes Involved in Lipid Synthesis in Young and Aged Mice. Genes involved in lipid metabolism were downregulated in PGAT of young and aged mice whereas SCAT of aged mice showed minor dysregulations of the respective genes. a) mRNA levels of fatty acid transporters in PGAT and SCAT of young and aged mice and b) mRNA levels of genes involved in lipid synthesis. Values represent the fold-change of the respective gene relative to cyclophilin reference gene by qPCR with endogenous gene expression in ATs of control mice (10 weeks) arbitrarily set to 1. Values are represented as average + SE. Significance between genotypes/different age was determined by student's t-test ($p \leq 0.05 = *$, $0.001 = ***$ / $p \leq 0.05 = \#$).

Together, determination of mRNA expression patterns demonstrated dysregulated AT function in AHKO mice, especially pronounced in PGAT depots, resulting in impaired AT expansion.

Consistent with dysregulations in lipid metabolism, infiltration of immune cells was significantly increased in both AT depots of AHKO mice at 24 weeks of age (**Figure 18**). Interestingly, AHKO PGAT exhibited increased infiltration already at 10 weeks of age. This recruitment of immune cells including macrophages indicate ongoing inflammatory processes within the AT depots.

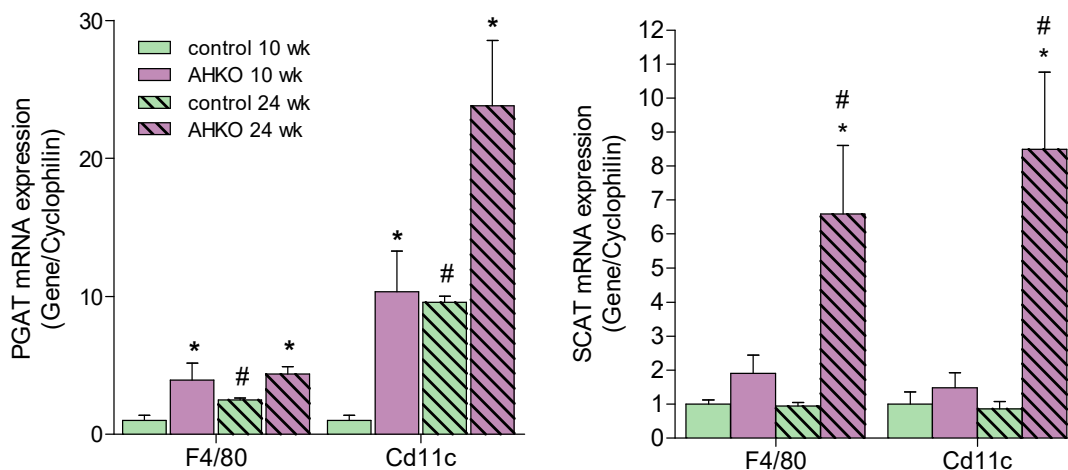


Figure 18: Immune Cell Infiltration in AT Depots of Control and AHKO Mice. Immune cell markers were significantly increased in 24-week-old AHKO mice in both AT depots. Immune cell infiltration in perigonadal AT was already increased at 10 weeks of age. a) mRNA levels in perigonadal AT (PGAT) and b) mRNA levels in subcutaneous AT (SCAT). Values represent the fold-change of the respective gene relative to cyclophilin reference gene by qPCR with endogenous gene expression in ATs of control mice (10 weeks) arbitrarily set to 1. Values are represented as average + SE. Significance between genotypes/different age was determined by student's t-test ($p \leq 0.05 = *$ / $p \leq 0.05 = \#$).

Together, these data demonstrate that the loss of HSL in adipocytes is accompanied with reduced ATGL and CGI-58 protein expression, indicating a downregulation of the complete lipolytic process. The reduced release of signaling molecules impairs lipid uptake, synthesis, and storage in AT. Furthermore, the decreased expression of PLIN1 suggests a reduced number of functional adipocytes in AHKO AT resulting in an induced inflammatory response.

Investigation of Systemic Glucose and Lipid Metabolism in AHKO mice

To investigate the impact of adipocyte HSL loss on systemic lipid and glucose homeostasis, we performed *in vivo* uptake with radiolabeled energy substrates in HFD fed AHKO and control mice. Glucose and fatty acid uptake were performed simultaneously within the same experiment. For this purpose, radiolabeled ^3H -2-Deoxyglucose was administered to the animals *via* intraperitoneal injection and ^{14}C -Bromo-Palmitate was injected intravenously with a delay of five minutes. The substrate uptake was observed over 10 (FA) and 15 minutes (glucose), respectively.

As expected, the liver, as central metabolic organ, incorporated the highest amount of the provided substrates. However, the uptake of FA into the liver was significantly reduced (~40%) in AHKO mice compared to wildtype littermates, which was rather unexpected, as our group and previous studies showed that AHKO mice develop a fatty liver over time [40]. Furthermore, the uptake of Bromo-Palmitate was significantly reduced in PGAT (-60%) and cardiac muscle (-35%) while the other tissues showed no differences between the genotypes but are tendential reduced in AHKO mice (**Figure 19a**).

Interestingly, glucose uptake into the liver tended also to be impaired in AHKO mice. Further analysis of tissue lysates revealed no significant differences regarding glucose uptake between control and KO animals in WAT, BAT, and cardiac muscle, but was significantly in skeletal muscle (**Figure 19b**).

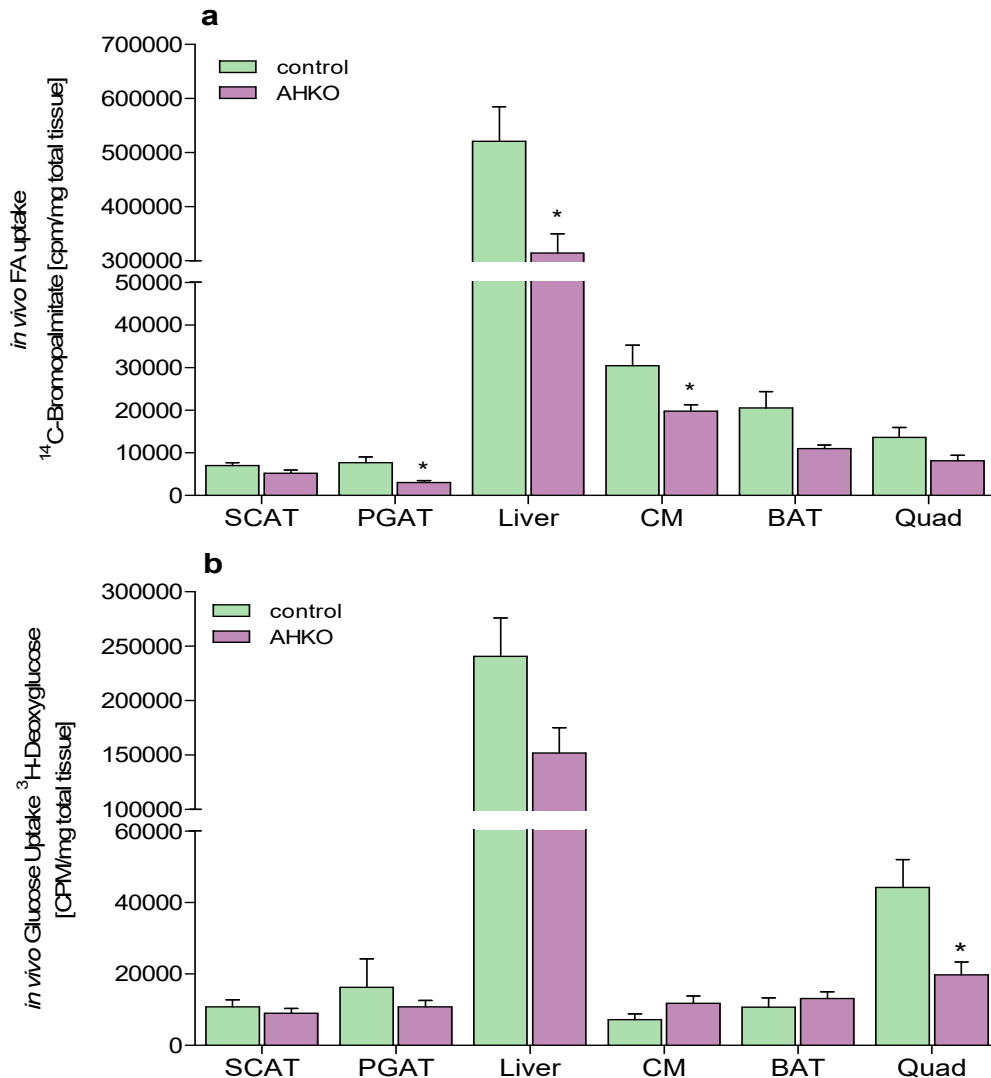


Figure 19: In Vivo Fatty Acid and Glucose Uptake. Fatty acid uptake was reduced in PGAT, Liver, and cardiac muscle of AHKO mice. AT depots did not show significant differences in glucose uptake between genotypes. However, glucose uptake was reduced in skeletal muscle a) Uptake of radiolabeled ¹⁴C-Bromo-Palmitate (BP) in several tissues of control and AHKO mice. Mice were fasted for 6h and BP (1 μ Ci/mouse) was administered via the retroorbital plexus. (b) Uptake of radiolabeled ³H-Deoxyglucose in several tissues of control and AHKO mice. Mice were fasted for 6h and 2-deoxyglucose (10 μ Ci/mouse) was administered intraperitoneally. Values are normalized to total tissue weight and are illustrated as average + SE. Significance was determined by student's t-test ($p \leq 0.05 = *$).

Another important aspect of *in vivo* lipid metabolism is the uptake of lipids in form of lipoproteins including chylomicrons and VLDL. Therefore, lipid uptake was performed using ³H-triolein within an olive oil gavage. Results revealed no differences in the accumulation of the substrate in the small intestine of AHKO and control animals, indicating a proper uptake of the substrate for further distribution (data not shown). Again, the uptake of lipids was the highest in the liver, which was comparable between control and AHKO animals. In addition, except for a minor decrease in BAT, AHKO

mice did not show alternations in the uptake of lipids after olive oil gavage, indicating functional lipoprotein formation and distribution (**Figure 20**).

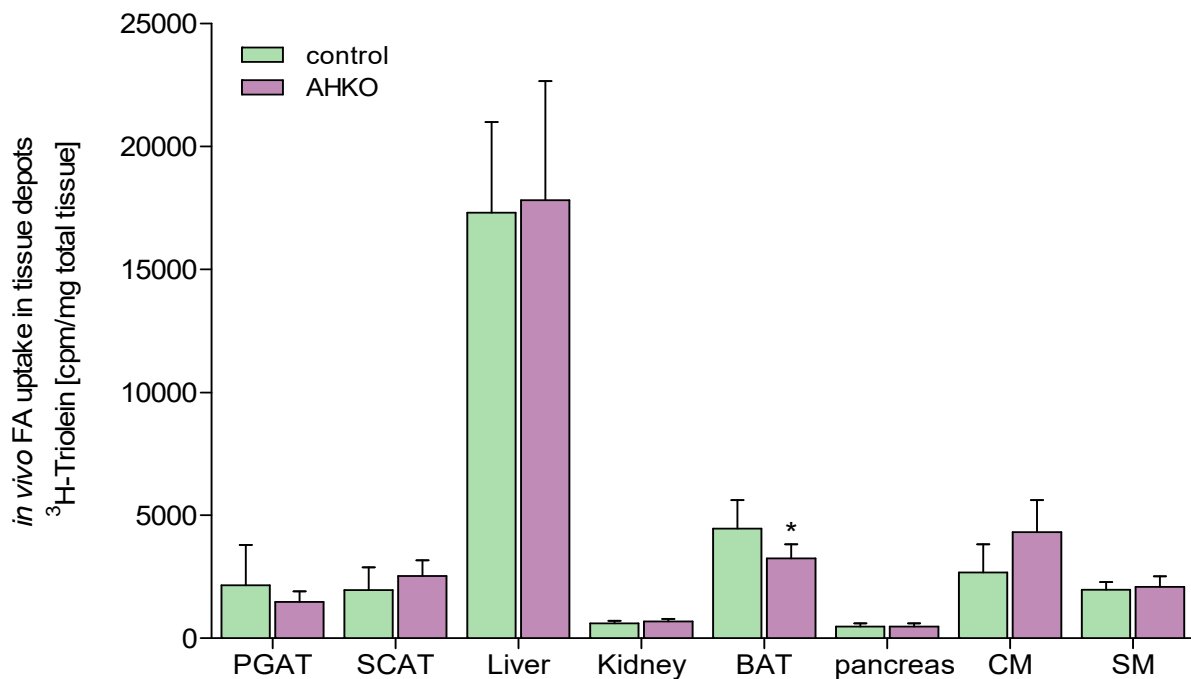


Figure 20: In Vivo Lipid Uptake of Triolein in Tissue Depots of Control and AHKO mice. The specific deletion of HSL in adipocytes was not accompanied with alternations in tissue fatty acid uptake after radiolabeled triolein gavage. Mice were fasted for 12 h and ^3H -triolein ($2\mu\text{Ci}/\text{mouse}$) was given via olive oil gavage. Values are normalized to total tissue weight and are illustrated as average + SE. Significance was determined by student's t-test ($p \leq 0.05 = *$)

In conclusion, AT depots of AHKO mice are characterized through progressively reduction in tissue expansion along with major dysregulations of AT metabolism. These dysregulations include an age dependent downregulation of important genes involved in adipocyte differentiation, lipid uptake and synthesis. Along with metabolic dysfunction, AT is infiltrated with immune cells indicating inflammatory processes within the tissues probably due to reduced number of healthy adipocytes. These devastating effects are especially pronounced in PGAT which is more lipolytic active. However, investigations on the cellular level of adipocyte metabolism did not show significant disadvantages for cells lacking HSL. This indicates that the loss of HSL might be compensated in the early stages of adipocyte lifetime. However, prolonged deletion of HSL is associated with major dysregulation of adipocyte function resulting in disruptions in AT metabolism and consequences on whole body homeostasis.

5. Discussion

Investigation of lipid metabolism and the underlying metabolic pathways build the foundation for a better understanding of pathogenesis of metabolic diseases like obesity or diabetes that represent major health risks of today's society. These non-communicable diseases are often associated with dysregulations in AT with either massive fat expansion or AT wasting leading to further pathogenesis including cardiomyopathy, hepatic steatosis, or cancer. This accredits AT an undisputable role to maintain systemic metabolic balance. Therefore, the understanding of AT function and its impact on non-AT metabolism is crucial to develop new strategies to treat these metabolic diseases.

AT provides the largest energy reservoir of the body with FAs being stored in form of TAGs in specialized compartments of adipocytes. Lipolysis, the breakdown of TAGs to NEFAs and glycerol, is a highly regulated process, depending on numerous enzymes, signaling molecules as well as dietary status. The main lipases found in AT are ATGL and HSL catalyzing the first and second step of lipolysis, respectively [33]. The systemic deletion of ATGL in mice leads to a severe accumulation of TAG within various tissues resulting in lethal cardiomyopathy [24]. However, ATGL-KO mice are glucose tolerant and insulin sensitive. Likewise, impaired adipocyte ATGL activity was also associated with beneficial effects on systemic homeostasis including glucose tolerance and insulin sensitivity [29], [30]. Although, HSL-KO mice are resistant to diet-induced obesity, the systemic HSL knockout is associated with major health problems in both humans and mice including accumulation of DAG species along with increasing risk of type 2 diabetes and the development of fatty liver disease [37], [40], [41], [51]. Adipose tissue specific deletion of HSL using the adipose protein 2 (*Ap2*) promoter is associated with glucose intolerance and the development of fatty liver mice. In contrast, liver specific knockout of HSL does not induce these complications [40]. However, underlying mechanisms of AT/non-AT cross talk are still unknown.

Since the *Ap2* promoter has been shown to stimulate gene deletion also in non-AT and different cell types including preadipocytes and macrophages [52], we characterized mice expressing Cre recombinase under control of the mouse adiponectin (*AdipoQ*) promoter. Adiponectin is predominantly expressed during the late phase of adipocyte differentiation resulting in a specific deletion of HSL in mature adipocytes. With this study we investigated the contribution of adipocyte specific HSL deletion on AT development and function and its consequences on non-AT and systemic glucose and lipid metabolism *in vivo*.

To get a better understanding of the role of adipocyte HSL on the underlying mechanisms it is important to start the investigation on the cellular level of adipocyte. Primary cells provide a powerful tool for this purpose as they are directly isolated from AT depots of the respective knockout animals. The differentiation of pluripotent preadipocytes to mature adipocytes is the initial process to provide normal AT function. Adipogenesis is characterized through changes within the expression pattern of genes that are responsible for the development of the adipocyte phenotype. This process requires the activation of a network of transcription factors with *Ppar γ* as key regulator [10]. *Ppar γ* is the most abundant member of the PPAR-superfamily in AT and various genes that are involved in characteristic AT functions including lipid uptake and synthesis (*Cd36*, *aP2*, *Pepck*) are known *Ppar γ* targets [12], [17]. Transcription factors from the *C/ebp* superfamily and *Srebp1c* are known co-activators of *Ppar γ* either by inducing its gene expression or providing ligands for binding [12].

Adipocyte differentiation experiments indicated that AHKO AT provides healthy preadipocytes with sufficient expression of important transcription factors and proper storage of neutral lipids resulting in mature adipocytes. However, the increase of adiponectin expression and the associated deletion of HSL occurred only at the late phase of adipogenesis. HSL deletion was detectable at day 4, when the expression of the key regulator *Pparγ* had already increased drastically (~400%). Therefore, a possible effect of HSL deficiency on adipogenesis might be suppressed as the differentiation process was already initiated through the expression of *Pparγ* and other transcription factors. Similar to our results, studies in primary cells isolated from HSL haploinsufficient mice revealed a normal cell development and differentiation capacity. In contrast, cells from HSL null animals displayed a delay in adipocyte differentiation [53], indicating that the loss of HSL at the early phase of differentiation affects adipogenesis. In contrast, despite enhanced lipid accumulation, the deletion of ATGL did not have any consequences on the differentiation process [54]. Whereas, it was shown that knockdown of GOS2, a known inhibitor protein of AGTL, reduced adipogenic capacity [54].

The total amount of accumulated neutral lipids was not altered between control and knockout cells during the differentiation process. Both cell types showed a decrease in neutral lipid content at day two before a continual increase within the last phase of differentiation. This decrease might be due to an initial reduction in CE species as shown *via* thin layer chromatography or to a possible growth arrest of cells after the initiation of the differentiation process as reported before [12]. In addition to total lipid content, differences in accumulated lipid species were not detectable in primary adipocytes. Although, quantification of the signal revealed a tendentially increase in TAGs and 1,2- DAG species from day 4 onward in cells lacking HSL. However, studies in mice with the systemic deletion of HSL found massive accumulation of DAG in various tissues [37]. In contrast, our primary cells isolated from SCAT of AHKO mice did not show significant differences in DAG accumulation during adipogenesis, suggesting impaired lipolytic activity in AHKO adipocytes. Accordingly, previous data from our lab showed a reduced lipolytic activity of primary adipocytes lacking HSL both under basal and isoproterenol stimulated conditions.

Together, our results indicate that HSL is not required during the last phase of adipocyte differentiation. Cells isolated from AHKO mice did not show disadvantages regarding neutral lipid accumulation and the expression of transcription factors that are responsible for a successful differentiation process. Although HSL expression drastically increased not until the late phase of adipocyte differentiation, we cannot exclude that HSL is also critical in the early phase of this process.

Adipocyte function is characterized through the ability of lipid uptake, storage, and release as well as insulin sensitivity to enhance glucose uptake upon nutritional abundance. As we could not observe differences in the cellular appearance and the differentiation process from pluripotent cells to mature adipocytes, we further investigated adipocyte function.

The cellular uptake of FFA can either be driven through diffusion or the contribution of FA transporters such as *Cd36* and *Fabp4* [20]. Bromo-Palmitate is a synthetic compound that cannot be further metabolized within the cell. Therefore, the measurement of intracellular radiolabeled lipid content directly reflects the FA uptake from the media. In contrast, oleic acid provides a substrate that can be further processed within the cell, including TAG synthesis, lipolysis, and FA release. Both experiments revealed no differences in FA uptake into primary cells between KO and control cells, indicating a proper response to FA availability and the transport into the cell. In addition to basal conditions, we treated the cells with insulin to promote FA uptake. However, a positive effect on FA uptake could not be observed neither in control nor in AHKO cells.

Glucose uptake in cells is promoted through special proteins, enabling the transport of extracellular glucose within the cell. The predominantly expressed glucose transporter in adipocytes is GLUT4. Under basal conditions, GLUT4 is mainly present in its inactive form within the cytosol. Insulin stimulation causes the translocation and the fusion of the transporter with the cell membrane to facilitate glucose uptake. The expression analysis of *Glut 4* in mature adipocytes revealed a significant increase of mRNA levels in cells derived from AHKO mice compared to control animals. However, measurements of intracellular glucose uptake did not show increased uptake in AHKO adipocytes. These contrary results indicate that the expression of *Glut4* on mRNA level might not correlate with its protein level or activity. Thus, impaired RNA processing, protein activity or proper translocation of the protein to the cell membrane cannot be excluded. However, the upregulation of gene expression might be an attempt of the cell to cope with HSL loss and its accompanied reduced release of lipid molecules.

Cellular glucose uptake is enhanced through increasing insulin levels, acting through a signaling cascade on the activity of insulin sensitive glucose transporters. However, insulin stimulated glucose uptake was increased in both wildtype and KO cells, indicating a functional reaction to insulin at least for glucose metabolism. Furthermore, the signaling molecule AKT was phosphorylated upon insulin treatment in both preadipocytes and adipocytes suggesting no differences in signal transduction upon insulin stimulated glucose uptake between control and KO cells. In contrast, previous studies in primary cells from haploinsufficient HSL mice [53] and human multipotent adipose-derived stem cells (hMADS) with reduced HSL expression (downregulation of HSL expression up to 60%) [55] found a positive correlation between reduced HSL activity and increased glucose uptake and insulin sensitivity. However, these observations could not be confirmed in our primary AHKO adipocytes since these cells did not display improved insulin signaling and glucose uptake compared to control cells. These data suggest that knockdown of HSL has a more beneficial impact on cellular glucose homeostasis than complete loss of HSL.

Interestingly, intracellular glucose uptake in preadipocytes was decreased in cells derived from AHKO mice compared to control cells. However, at this stage of differentiation, HSL expression is not altered between the cells since adiponectin expression is very low in preadipocytes. Therefore, the decreased glucose uptake was not caused by HSL deletion. A reason for the reduced uptake might be the different composition of cell types within the SVC, since AHKO AT contains more immune cells compared to control AT.

Although, the results obtained from primary cells indicated that HSL loss is not accompanied with impaired differentiation and metabolic dysfunctions, these observations cannot be directly translated to AT health and function in mice. Previously it was shown that alternations in AT HSL are associated with the development of lipodystrophic AT depots in mice fed a standard chow diet [40]. To investigate whether this was also true in our adipocyte specific HSL mouse model in the setting of high caloric input, we fed AHKO mice HFD for more than 20 weeks and evaluated their AT phenotype.

AHKO mice showed similar body weight and fat mass within the first weeks of HFD feeding, but KO mice progressively gained less body weight and fat mass with age. The reduction of total fat mass in AHKO mice was accompanied with a stagnation in AT expansion in both SCAT and PGAT of 24-week-old animals. All observations, including the macroscopic changes in AT appearance and metabolic observations were more pronounced in PGAT. This is interesting as visceral AT was found to be more critically involved in the development of diabetes and cardiovascular diseases than SCAT depots. This is due to differences arising from AT location, variations in cell type composition, lipolytic activity, and the expression pattern of β -adrenergic receptors, which is more pronounced in visceral AT depots [13] [4]. In contrast to WAT depots, weight of the intrascapular BAT depot increased in AHKO mice. This

observation was also found in AAKO animals, where the increase was associated with morphological changes causing a 'whitening' effect in BAT [29]. However, the function role of HSL in BAT is still elusive and additional studies are required to evaluate its metabolic contribution.

The hydrolysis of TAGs to release FFA and glycerol is a fundamental process for both AT and non-AT function as FFA serve as substrate for energy production and provide important signaling molecules and building blocks for biological membranes and further metabolites. Thereby, HSL and ATGL represent the main lipases in AT [33] with HSL showing the highest affinity for catalyzing DAG species. Our results showed a significant reduction in lipolytic activity of WAT depots *ex vivo* (*data not shown*) and reduced circulating plasma NEFA and glycerol levels in mice lacking adipocyte HSL in the fasted, but not fed state. ATGL and its co-activator CGI-58 protein expression were drastically downregulated in AHKO WAT starting at 10 weeks of age and resulting in a reduction of their expression to less than 20% in aged mice. Whether the downregulation of major lipolytic proteins is a compensatory mechanism to reduce DAG accumulation within the tissue depots or whether there are other reasons for the reduced expression cannot be answered at this time of study. However, despite reduced lipolytic activity due to HSL loss and reduced expression of ATGL and CGI-58, AT mass of AHKO mice did not increase, indicating that lipolysis is a crucial process to maintain AT function such as lipid synthesis and storage [29], [56]. According to alternations in lipolytic activity, key enzymes regulating fundamental lipid metabolic processes, including adipogenesis, lipid uptake, and synthesis were significantly downregulated in WAT depots of AHKO mice. This supports the assumption that HSL is not only important for TAG breakdown in terms of energy supply but also involved in the provision of ligands or precursor molecules for PPAR γ signaling which regulates critical processes of lipid metabolism.

To better understand the importance of adipocyte specific HSL to systemic metabolism, we further investigated substrate uptake into different tissues *in vivo*. Previous studies in mice with systemic deletion [24] or an adipocyte specific deletion of ATGL (AAKO) [29] demonstrated that reduced supply with FAs alters their systemic substrate utilization for energy production from lipid to carbohydrate. Furthermore, knockdown of HSL increased *in vivo* glucose uptake into AT, thereby improving AT and systemic glucose metabolism [55]. However, these changes were not observed in our animals, as AHKO mice showed only minor alternations in systemic glucose or FA uptake. *In vivo* uptake of glucose did not reveal significant differences between AHKO and control mice in AT while FA uptake was only mildly reduced, suggesting "more or less" normal uptake of nutrients from AT depots of AHKO mice.

Remarkably, although our AHKO mice massively accumulated TAG within the liver (*data not shown*) resulting in hepatic steatosis in aged KO mice, the uptake of glucose and FAs was unaltered or even tended to be decreased in the liver of AHKO mice. These data suggest that fatty liver is not due to alternations in substrate uptake but rather caused by other mechanisms such as increased *de novo* lipogenesis. Interestingly, the deletion of adipocyte specific ATGL causes the opposite effect on the liver, preventing fatty liver development in AAKO mice [29]. Together, the loss of adipocyte HSL impairs adipocyte function and consequently non-AT lipid metabolism. However, the changes in AHKO mice are not primarily caused by alteration in substrate uptake. Therefore, the metabolic processes responsible for the dysregulations are still elusive.

Obesity is closely associated with adipocyte death and immune cell infiltration into AT depots in both humans and mice [57] [58]. Macrophages are specialized immune cells that are part of the innate immune system and are involved in phagocytosis and inflammatory response. Despite reduced AT weight and resistance to diet induced obesity in our AHKO mice, AT depots were infiltrated with

immune cells, indicating inflammatory processes. Our observations were comparable to those in systemic HSL KO mice, where AT displayed immune cell infiltration along with necrosis, displaying pro-inflammatory adipocyte death. This is indicated by recruitment of macrophages to surround dead adipocytes to form crown like structures (CLS) [58]. Accordingly, AHKO AT exhibited, besides increased expression of immune cell markers, also reduced protein levels of PLIN1, indicating a reduction in healthy adipocytes in AHKO mice. Since, HSL and ATGL are major enzymes involved in lipid metabolism, changes in their activity causes an inflammatory response in AT. Deletion of adipocyte ATGL displays improvement in the acute immune response in AT [29]. However, long term deletion of adipocyte ATGL is not associated with beneficial effects in immune cell infiltration [29] and become more comparable to HSL-KO AT.

Overall, the AHKO mouse represents an interesting research model to investigate AT lipid metabolism and its contribution to systemic homeostasis. The results obtained during this master thesis contribute to a better understanding of adipocyte HSL to AT lipid metabolism and its consequences for systemic energy homeostasis. Our results indicate that the adipocyte specific loss of HSL has only minor impact on metabolic function on a cellular level. During this early stage of the adipocyte lifespan, cells might be able to compensate for HSL loss. The permanent loss of HSL, however, results in severe problems for the cells and in turn for AT and systemic homeostasis. In fact, the alternations in AT metabolism through the deletion of HSL in adipocytes is associated with consequences reaching beyond AT function. AHKO mice reveal lipodystrophic AT depots with mounting insulin resistance and the development of hepatic steatosis with age [40]. These results accredit HSL an important role in systemic metabolism properly through the ability of providing important substrates for processes including PPAR γ signaling. Furthermore, with this study we confirmed the importance of AT as an important tissue contributing to systemic health. Disruptions in AT balance are accompanied with pathogenesis reaching beyond AT function itself. However, further investigations of the cross talk between AT and ectopic tissues are required to determine the role of adipocyte specific HSL and the underlying mechanisms on systemic homeostasis. The phenotype of our mouse model clearly develops over time. Therefore, investigations of the progressive phenotype after 24 weeks of age are of importance. Unlike alternations in ATGL activity [29], [30] that are associated with beneficial effects for the individual, adipocyte specific deletion of HSL causes severe dysregulations in AT function, hepatic steatosis as well as increased immune cell infiltration and inflammation. Further studies will help to identify the contribution of adipocyte HSL to systemic metabolic homeostasis.

Abbreviations

AC	Adenylate cyclase	HSL	Hormone-sensitive lipase
ACC	Acyl-CoA-synthetase	IL-6	Interleukin 6
AdipoQ	Adiponectin	IRS	Insulin receptor substrate
AGPAT2	1-acylglycerol-3-phosphate O-acyltransferase 2	LD	Lipid droplet
AKT	Protein kinase B	LDL	Low-density lipoproteins
AT	Adipose Tissue	LPL	Lipoprotein lipase
ATGL	Adipose triglyceride lipase	MAG	Monoacylglyceride
ATP	Adenosine triphosphate	MGAT	Monoacylglycerol-acyltransferase
BAT	Brown adipose tissue	MGL	Monoacylglycerol lipase
BMI	Body mass index	mTORC	Mammalian target of rapamycin complex
C/EBPs	CCAAT/ enhancer-binding proteins	NEFA	Non-esterified fatty acid
cAMP	Cyclic adenosine monophosphate	PAP	Phosphatidic acid phosphohydrolase
CD36	Fatty acid translocase	PDK1	PIP3-dependent kinase
CE	Cholesteryl ester	PGAT	Perigonadal adipose tissue
CGI-58	Comparative gene identification protein 58	PIK3	Phosphoinositol kinase 3
CLS	Crown like structures		
DAG	Diacylglyceride	PIP3	Phosphatidylinositol-3,4,5-triphosphate
DGAT	Diacylglycerol-acyltransferase	PKA	Protein kinase A
FASN	Fatty acid synthase	PLIN 1	Perilipin 1
(F)FA	(Free) fatty acid	PPARs	Peroxisome proliferator-activated receptors
FATPs	Fatty acid transport proteins	RAAS	Renin-angiotensin-aldosterone-system
FGF-21	Fibroblast growth factor-21	RE	Retinyl ester
G0S2	G0/G1 switch protein-2	SCAT	Subcutaneous adipose tissue
G3P	Glycerol-3-phosphate	SREBP1c	Sterol regulatory binding protein
GLUT	Glucose transporter	SVC	Stromal-vascular cells
GPAT	Glycerol-3-phosphate-acyltransferase	TAG	Triacylglyceride
HDL	High-density lipoproteins	TNF α	Tumor necrosis factor α
HFD	High-fat diet	UCP1	Uncoupling protein 1
HLPDA	Hypoxia inducible lipid droplet-associated protein	VLDL	Very low-density lipoproteins
		WAT	White adipose tissue

References

- [1] "WHO- 10 facts on obesity." [Online]. Available: <https://www.who.int/news-room/fact-sheets/detail/the-top-10-causes-of-death>.
- [2] N. Kraemer, R. V. Farese, and T. C. Walther, "Balancing the fat: Lipid droplets and human disease," *EMBO Mol. Med.*, vol. 5, no. 7, pp. 905–915, 2013.
- [3] T. C. Walther and R. V. Farese, "Lipid Droplets and Cellular Lipid Metabolism," *Annu. Rev. Biochem.*, vol. 81, no. 1, pp. 687–714, 2012.
- [4] A. Wronska and Z. Kmiec, "Structural and biochemical characteristics of various white adipose tissue depots," *Acta Physiol.*, vol. 205, no. 2, pp. 194–208, 2012.
- [5] E. E. Kershaw and J. S. Flier, "Adipose tissue as an endocrine organ," *J. Clin. Endocrinol. Metab.*, vol. 89, no. 6, pp. 2548–2556, 2004.
- [6] B. M. Rosen, Evan D.; Spiegelman, "What we Talk About When We Talk About FAT," *J. Mod. Lit.*, vol. 41, no. 2, pp. 175–177, 2018.
- [7] S. Stock, M. J.; Cinti, "Adipose Tissue: Structure and Function of Brown Adipose Tissue," *Encycl. Food Heal.*, pp. 30–34, 2015.
- [8] J. Villarroya, R. Cereijo, A. Gavaldà-Navarro, M. Peyrou, M. Giralt, and F. Villarroya, "New insights into the secretory functions of brown adipose tissue," *J. Endocrinol.*, vol. 243, no. 2, pp. R19–R27, 2019.
- [9] M. Thuzar and K. K. Y. Ho, "Mechanisms in endocrinology: Brown adipose tissue in humans: Regulation and metabolic significance," *Eur. J. Endocrinol.*, vol. 175, no. 1, pp. R11–R25, 2016.
- [10] E. D. Rosen *et al.*, "PPAR γ is required for the differentiation of adipose tissue in vivo and in vitro," *Mol. Cell*, vol. 4, no. 4, pp. 611–617, 1999.
- [11] D. Moseti, A. Regassa, and W. K. Kim, "Molecular regulation of adipogenesis and potential anti-adipogenic bioactive molecules," *Int. J. Mol. Sci.*, vol. 17, no. 1, pp. 1–24, 2016.
- [12] B. M. Rosen, Evan D.; Walkey, Christopher J.; Spiegelman, "Transcriptional regulation of adipogenesis," *Compr. Physiol.*, vol. 7, no. 2, pp. 635–674, 2017.
- [13] E. D. Rosen and B. M. Spiegelman, "Molecular Regulation of Adipogenesis," *Gene*, 2000.
- [14] G. J. Darlington, S. E. Ross, and O. A. MacDougald, "The role of C/EBP genes in adipocyte differentiation," *J. Biol. Chem.*, vol. 273, no. 46, pp. 30057–30060, 1998.
- [15] T. Tanaka, N. Yoshida, T. Kishimoto, and S. Akira, "Defective adipocyte differentiation in mice lacking the C/EBP β and/or C/EBP δ gene," *EMBO J.*, vol. 16, no. 24, pp. 7432–7443, 1997.
- [16] "SREBF1 streol regulatory element binding transcription factor." [Online]. Available: https://www.ncbi.nlm.nih.gov/gene?cmd=Retrieve&dopt=full_report&list_uids=6720. [Accessed: 01-Dec-2019].
- [17] A. K. Hihi, L. Michalik, and W. Wahli, "PPARs: Transcriptional effectors of fatty acids and their derivatives," *Cell. Mol. Life Sci.*, vol. 59, no. 5, pp. 790–798, 2002.
- [18] N. Belmonte, C. Vernochet, and C. Dani, "PPAR gamma is required for placental, cardiac, and

- adipose tissue development," *Medecine/Sciences*, vol. 16, no. 2, pp. 253–254, 2000.
- [19] J. R. Jones *et al.*, "Deletion of PPAR γ in adipose tissues of mice protects against high fat diet-induced obesity and insulin resistance," *Proc. Natl. Acad. Sci. U. S. A.*, vol. 102, no. 17, pp. 6207–6212, 2005.
- [20] P. C. Heinrich, M. Müller, and L. Graeve, *Biochemie und Pathobiochemie*. 2014.
- [21] C. L. E. Yen, S. J. Stone, S. Koliwad, C. Harris, and R. V. Farese, "DGAT enzymes and triacylglycerol biosynthesis," *J. Lipid Res.*, vol. 49, no. 11, pp. 2283–2301, 2008.
- [22] C. A. Harris *et al.*, "DGAT enzymes are required for triacylglycerol synthesis and lipid droplets in adipocytes," *J. Lipid Res.*, vol. 52, no. 4, pp. 657–667, 2011.
- [23] S. J. Stone *et al.*, "Lipopenia and Skin Barrier Abnormalities in DGAT2-deficient Mice," *J. Biol. Chem.*, vol. 279, no. 12, pp. 11767–11776, 2004.
- [24] G. Haemmerle *et al.*, "Triglyceride Lipase," vol. 211, no. May, pp. 734–738, 2006.
- [25] A. Lass *et al.*, "Adipose triglyceride lipase-mediated lipolysis of cellular fat stores is activated by CGI-58 and defective in Chanarin-Dorfman Syndrome," *Cell Metab.*, vol. 3, no. 5, pp. 309–319, 2006.
- [26] R. Zechner, "FAT FLUX: enzymes, regulators, and pathophysiology of intracellular lipolysis," *EMBO Mol. Med.*, vol. 7, no. 4, pp. 359–362, 2015.
- [27] K. M. Padmanabha Das *et al.*, "Hypoxia-inducible lipid droplet-associated protein inhibits adipose triglyceride lipase," *J. Lipid Res.*, vol. 59, no. 3, pp. 531–541, 2018.
- [28] X. L. Yang *et al.*, "G0/G1 Switch Gene 2 Regulates Adipose Lipolysis through Association with Adipose Triglyceride Lipase," *Bone*, vol. 23, no. 1, pp. 1–7, 2008.
- [29] G. Schoiswohl *et al.*, "Impact of reduced ATGL-mediated adipocyte lipolysis on obesity-associated insulin resistance and inflammation in male mice," *Endocrinology*, vol. 156, no. 10, pp. 3610–3624, 2015.
- [30] P. Kotzbeck *et al.*, "Pharmacological inhibition of adipose triglyceride lipase corrects high-fat diet-induced insulin resistance and Hepatosteatosis in Mice," no. May 2016, 2017.
- [31] F. P. W. Radner *et al.*, "Growth retardation, impaired triacylglycerol catabolism, hepatic steatosis, and lethal skin barrier defect in mice lacking comparative gene identification-58 (CGI-58)," *J. Biol. Chem.*, vol. 285, no. 10, pp. 7300–7311, 2010.
- [32] J. M. Brown *et al.*, "CGI-58 knockdown in mice causes hepatic steatosis but prevents diet-induced obesity and glucose intolerance," *J. Lipid Res.*, vol. 51, no. 11, pp. 3306–3315, 2010.
- [33] M. Schweiger *et al.*, "Adipose triglyceride lipase and hormone-sensitive lipase are the major enzymes in adipose tissue triacylglycerol catabolism," *J. Biol. Chem.*, vol. 281, no. 52, pp. 40236–40241, 2006.
- [34] J. A. Rodriguez *et al.*, "In vitro stereoselective hydrolysis of diacylglycerols by hormone-sensitive lipase," *Biochim. Biophys. Acta - Mol. Cell Biol. Lipids*, vol. 1801, no. 1, pp. 77–83, 2010.
- [35] A. Lass, R. Zimmermann, M. Oberer, and R. Zechner, "Lipolysis - A highly regulated multi-enzyme complex mediates the catabolism of cellular fat stores," *Prog. Lipid Res.*, vol. 50, no. 1, pp. 14–27, 2011.

- [36] "UNIPROT." [Online]. Available: <https://www.uniprot.org/uniprot/Q05469#function>.
- [37] G. Haemmerle *et al.*, "Hormone-sensitive lipase deficiency in mice causes diglyceride accumulation in adipose tissue, muscle, and testis," *J. Biol. Chem.*, vol. 277, no. 7, pp. 4806–4815, 2002.
- [38] K. Harada *et al.*, "Resistance to high-fat diet-induced obesity and altered expression of adipose-specific genes in HSL-deficient mice," *Am. J. Physiol. - Endocrinol. Metab.*, vol. 285, no. 6 48-6, pp. 1182–1195, 2003.
- [39] P. Morigny, M. Houssier, E. Mouisel, and D. Langin, "Adipocyte lipolysis and insulin resistance," *Biochimie*, vol. 125, pp. 259–266, 2016.
- [40] B. Xia, G. H. Cai, H. Yang, S. P. Wang, G. A. Mitchell, and J. W. Wu, "Adipose tissue deficiency of hormone-sensitive lipase causes fatty liver in mice," *PLoS Genet.*, vol. 13, no. 12, pp. 1–17, 2017.
- [41] C. Sztalryd *et al.*, "Null Mutation in Hormone-Sensitive Lipase Gene and Risk of Type 2 Diabetes," *N. Engl. J. Med.*, vol. 370, no. 24, pp. 2307–2315, 2014.
- [42] U. Taschler *et al.*, "Monoglyceride Lipase Deficiency in Mice Impairs Lipolysis and Attenuates Diet-induced Insulin Resistance * □," vol. 286, no. 20, pp. 17467–17477, 2011.
- [43] S. M. Choi *et al.*, "Insulin Regulates Adipocyte Lipolysis via an Akt-Independent Signaling Pathway," *Mol. Cell. Biol.*, vol. 30, no. 21, pp. 5009–5020, 2010.
- [44] P. Chakrabarti, T. English, J. Shi, C. M. Smas, and K. V. Kandror, "Mammalian target of rapamycin complex 1 suppresses lipolysis, stimulates lipogenesis, and promotes fat storage," *Diabetes*, vol. 59, no. 4, pp. 775–781, 2010.
- [45] M. Coelho, T. Oliveira, and R. Fernandes, "Biochemistry of adipose tissue: An endocrine organ," *Arch. Med. Sci.*, vol. 9, no. 2, pp. 191–200, 2013.
- [46] N. Maeda *et al.*, "Diet-induced insulin resistance in mice lacking adiponectin/ACRP30," *Nat. Med.*, vol. 8, no. 7, pp. 731–737, 2002.
- [47] C. S. Mantzoros *et al.*, "Leptin in human physiology and pathophysiology," *Am. J. Physiol. - Endocrinol. Metab.*, vol. 301, no. 4, 2011.
- [48] T. P. Zanto, K. Hennigan, M. Östberg, W. C. Clapp, and A. Gazzaley, "NIH Public Access," vol. 46, no. 4, pp. 564–574, 2011.
- [49] M. Sekiya *et al.*, "Absence of Hormone-sensitive Lipase Inhibits Obesity and Adipogenesis in Lepob/ob Mice," *J. Biol. Chem.*, vol. 279, no. 15, pp. 15084–15090, 2004.
- [50] A. Lass *et al.*, "Adipose triglyceride lipase-mediated lipolysis of cellular fat stores is activated by CGI-58 and defective in Chanarin-Dorfman Syndrome," *Cell Metab.*, vol. 3, no. 5, pp. 309–319, 2006.
- [51] F. B. Kraemer and W. J. Shen, "Hormone-sensitive lipase knockouts," *Nutr. Metab.*, vol. 3, pp. 1–7, 2006.
- [52] E. Jeffery *et al.*, "Characterization of Cre recombinase models for the study of adipose tissue," *Adipocyte*, vol. 3, no. 3, pp. 206–211, 2014.
- [53] R. Burcelin *et al.*, "Partial Inhibition of Adipose Tissue Lipolysis Improves Glucose Metabolism and Insulin Sensitivity Without Alteration of Fat Mass," *PLoS Biol.*, vol. 11, no. 2, p. e1001485, 2013.

- [54] H. Choi *et al.*, "G0/G1 switch gene 2 has a critical role in adipocyte differentiation," *Cell Death Differ.*, vol. 21, no. 7, pp. 1071–1080, 2014.
- [55] P. Morigny *et al.*, "Interaction between hormone-sensitive lipase and ChREBP in fat cells controls insulin sensitivity," *Nat. Metab.*, vol. 1, no. 1, pp. 133–146, 2019.
- [56] E. P. Mottillo, P. Balasubramanian, Y. H. Lee, C. Weng, E. E. Kershaw, and J. G. Granneman, "Coupling of lipolysis and de novo lipogenesis in brown, beige, and white adipose tissues during chronic β 3-adrenergic receptor activation," *J. Lipid Res.*, vol. 55, no. 11, pp. 2276–2286, 2014.
- [57] K. J. Strissel *et al.*, "Adipocyte death, adipose tissue remodeling, and obesity complications," *Diabetes*, vol. 56, no. 12, pp. 2910–2918, 2007.
- [58] S. Cinti *et al.*, "Adipocyte death defines macrophage localization and function in adipose tissue of obese mice and humans," *J. Lipid Res.*, vol. 46, no. 11, pp. 2347–2355, 2005.